Adaptive Fuzzy Control for Stochastic Nonlinear Systems with Non-Monotonic Prescribed Performance and Unknown Control Directions

Yu Xia, *Member, IEEE,* Zsófia Lendek, *Member, IEEE,* Zhibo Geng, Junyang Li, and Jiaxu Wang

***Abstract*—This paper presents an adaptive fuzzy control scheme capable of guaranteeing prescribed performance for stochastic nonlinear systems with unknown control directions. Unlike the majority of existing prescribed performance control schemes, the proposed scheme ensures the independence from initial errors and guarantees controllable overshoot. Moreover, the proposed prescribed function exhibits non-monotonicity, which can be beneficial in control applications with input constraints. To address the challenge posed by unknown control directions, a novel class of multiple Nussbaum functions is introduced. Compared to the existing single Nussbaum function, the multiple Nussbaum functions can mitigate instability arising from the cancellation of multiple unknown signs. Additionally, to tackle unknown nonlinearities, a single-parameter fuzzy approximator is introduced, aiming to concurrently reduce computational complexity. Furthermore, a novel class of switching threshold event-triggered mechanisms is designed to address issues encountered in existing designs where parameter inequalities impose conservative constraints. The control scheme ensures that the tracking error converges to prescribed asymmetric boundaries with arbitrarily small residuals in a prescribed time, while also guaranteeing that all closed-loop signals are bounded in probability. The effectiveness and superiority of the control scheme are verified by simulation results.**

***Index*—Stochastic nonlinear system, adaptive fuzzy control, non-monotonic prescribed performance, unknown control direction, event-triggered mechanism.**

The work was supported in part by the National Natural Science Foundation of China under Grant 52375041, and in part by the project DECIDE, funded under the PNRR I8 scheme by the Romanian Ministry of Research, Innovation and Digitisation, under Grant 57/14.11.2022. (Corresponding author: Yu Xia and Zsófia Lendek.)

Yu Xia is with the State Key Laboratory of Mechanical System and Vibration, Shanghai Jiao Tong University, Shanghai 200240, China, and also with the State Key Laboratory of Mechanical Transmission for Advanced Equipment, Chongqing University, Chongqing 400044, China (e-mail: rainyx@sjtu.edu.cn).

Zsófia Lendek is with the Department of Automation, Technical University of Cluj-Napoca; Memorandumului 28, 400114, Cluj-Napoca, Romania (e-mail: zsofia.lendek@aut.utcluj.ro).

Zhibo Geng is with the College of Aeronautics and Astronautics, University of Electronic Science and Technology of China, Chengdu, Sichuan 611731, China (e-mail: gzbgeng@uestc.edu.cn).

Junyang Li and Jiaxu Wang are with the State Key Laboratory of Mechanical Transmission for Advanced Equipment, Chongqing University, Chongqing 400044, China (e-mails: junyangli@cqu.edu.cn; profwjx@163.com).

I. Introduction

Control schemes designed for nonlinear systems are typically based on deterministic models [1]–[6]. However, practical engineering systems often experience the influence of stochastic factors from their external environment. As a result, there is a growing interest in developing control schemes for stochastic models. However, the existing literature [7]–[10] on control schemes for stochastic models has limited practical applicability due to infinite settling times. To address this issue, finite-time (FnT) and fixed-time (FxT) control schemes [11]–[14] have been developed for stochastic nonlinear systems based on the FnT [15] and FxT Lyapunov theory [16], respectively. The distinction between FxT and FnT control lies in the utilization of odd-order and fractional-order feedback by FxT control to shape the dynamic characteristics of the closed-loop system and estimate an upper bound of the settling time independently of initial conditions. This capability provides FxT control with an edge over FnT control. However, the upper bound of the settling time under FxT control is often overestimated, potentially several hundred to several thousand times, leading to an inaccurate description of system performance. On the other hand, whether FnT or FxT control, settling time is not a directly tunable parameter as it also depends on other design parameters of the controller. To address the issue of overestimation of settling time and reduce its dependency on design parameters, a predefined-time (PdT) control approach has been proposed for stochastic nonlinear systems in [17]. This method allows for setting a minimum upper bound on settling time without considering initial conditions or any other design parameters.

In recent years, the classic concept of prescribed-time (PT) control derived from the application of strategic tactical missile guidance [18] has been re-explored and further applied to control for stochastic nonlinear systems [19]. It inherits the advantages of FnT, FxT, and PdT control, allowing for the precise presetting of settling time. This concept is crucial in many practical engineering applications where transient processes must occur within a given time, such as missile guidance, emergency braking, and multi-agent rendezvous. In addition, a unique prescribed function known as the time-varying scaling function distinguishes PT control [19]–[22] from commonly used prescribed functions in [23]–[25]. This is due to its three key advantages: (1) it eliminates the constraint of initial conditions, meaning there is no need to redesign the performance function when the initial data changes; (2) its asymmetry allows for the adjustment of output overshoot; and (3) it enables precise design of settling time without requiring information about the minimum upper bound. However, in the referenced literature [19]–[22], the time-varying scaling function is defined as a strictly decreasing function over time. This monotonicity can sometimes be disadvantageous, as in certain practical scenarios a non-monotonic function might be more beneficial. For instance, as noted in [26], when dealing with highly fluctuating reference signals or periodic disturbances, extending the performance boundaries over a specific time span can be advantageous. Therefore, developing a time-varying scaling function with non-monotonic characteristics is of considerable interest.

Another interesting topic revolves around control problems under unknown control directions, with the common solution being the introduction of a Nussbaum function $N(\chi)$ [21], [27]–[30], used as a tool for control entities, as it can change its sign when χ varies to find the correct control direction. However, in [21], [27]–[30], the Nussbaum function is considered for a single control direction and it will no longer be applicable when there are multiple unknown time-varying control coefficients in the control system. The primary obstacle lies in the incapacity to accommodate multiple Nussbaum functions in a single Lyapunov inequality. To this end, a new type of Nussbaum functions $N_i(\chi)$ was proposed in [31]–[33] by considering the interconnection of multiple Nussbaum functions, thereby enabling the incorporation of multiple Nussbaum functions in a single Lyapunov inequality. However, the aforementioned methods [31]—[33] are based on the design and stability analysis of deterministic systems, and cannot be directly applied to stochastic nonlinear systems. Furthermore, these methods require prior knowledge of system parameters when selecting $N_i(\chi)$. In other words, employing multiple Nussbaum functions $N_i(\chi)$ for the design and stability analysis of stochastic systems remains an open issue.

At the same time, addressing communication network limitations within control systems has become a major concern in recent years. Extensive research [34]–[38] has been conducted on the event-triggered mechanism (ETM) as a viable solution to optimize communication network usage and enhance efficiency. Typically, the ETM is primarily based on fixed, relative, or switching threshold strategies. However, meticulous parameter selection is indispensable for all these strategies to ensure compliance with specific inequality restrictions, thus imbuing them with a degree of conservatism. Therefore, developing an event-triggered strategy that can overcome this limitation remains a challenging issue.

Building upon the preceding discussion, the control challenge persists for stochastic nonlinear systems with prescribed performance and unknown control directions. In response, we propose a novel control scheme that brings forth three key contributions.

(1) This paper proposes a class of prescribed performance functions with non-monotonic characteristics. In addition to the advantages highlighted in references [19]–[22], the proposed performance bounds exhibit non-monotonicity, which further relaxes performance requirements and expands the performance boundaries. This non-monotonicity offers greater generality and practicality in certain applications, such as in [39], [40], where control expenses may arise during input saturation or when switching from a faulty actuator to a backup actuator. In such cases, the use of a non-monotonic prescribed performance function has a positive influence.

(2) This paper proposes a novel class of Nussbaum functions, enabling the quantification of the interconnection of multiple Nussbaum functions in a single inequality. This method overcomes the limitation in references [21], [27]–[30] where accommodating these functions was not feasible. In addition, the Nussbaum functions designed in this article can be applied to stochastic nonlinear systems, addressing the limitation of previous methods [31]-[33] which were solely focused on deterministic systems. Therefore, the newly introduced Nussbaum functions offers significant convenience for designing controllers for stochastic nonlinear systems with unknown time-varying coefficients.

(3) This paper proposes a novel ETM that effectively addresses the challenge of inequality constraints commonly encountered in designing ETM parameters, as observed in references [34]–[38]. Additionally, by incorporating switching thresholds, this newly proposed ETM achieves a desirable trade-off between control performance and event frequency. Consequently, it significantly simplifies parameter adjustments and exhibits promising prospects for practical applications.

II. Problem Formulation and Preliminaries

A. System Model and Control Objective

Consider the uncertain stochastic nonlinear systems with unknown control directions as follows:

$$\begin{cases} dx_i = \left[b_i(t)\, x_{i+1} + f_i(\bar{x}_i)\right] dt + g_i^T(\bar{x}_i)\, d\omega, \\ \qquad 1 \le i \le n-1, \\ dx_n = \left[b_n(t)\, u + f_n(x)\right] dt + g_n^T(x)\, d\omega, \\ y = x_1, \end{cases} \tag{1}$$

where $\bar{x}_i = [x_1, x_2, \ldots, x_i]^T \in \mathbb{R}^i$ and $x = [x_1, x_2, \ldots, x_n]^T \in \mathbb{R}^n$ are the system vectors, y denotes the controlled output, u denotes the control input, $b_i(t) \neq 0, i = 1, 2, \ldots, n$ denote the unknown time-varying control coefficients, $f_i(\bar{x}_i)$ and $g_i(\bar{x}_i)$ are the unknown smooth functions, and ω denotes the standard Brownian motion.

Control Objective: Develop an adaptive fuzzy control algorithm for system (1), ensuring that all signals within the closed-loop system remain bounded in probability. Additionally, the tracking error should always evolve within predefined boundaries.

B. Non-Monotonic Prescribed Performance Function

To guarantee the non-monotonic prescribed performance concerning the tracking error, the following non-monotonic rate function is designed:

$$r(t) = \begin{cases} \left(\frac{T-t}{T}\right)^{a+1} \cos^2(t), 0 \le t < T, \\ 0, t \ge T, \end{cases} \tag{2}$$

where $a > 0$ and $T > 0$ are some constants.

From (2), $r(t)$ has the following properties: (1) $r(t) = 1, t = 0$; (2) $r(t) \in [0, 1), \forall t > 0$; and (3) $\dot{r}(t)$ is known, bounded, and piece-wise continuous.

Together with the aforementioned non-monotonic rate functions, we propose the non-monotonic prescribed performance function as follows:

$$\mathcal{P}(\rho) = \frac{l\rho(t)}{\sqrt{1 - \rho^2(t)}}, \tag{3}$$

where $l > 0$ denotes a constant, $\rho(t) = (\rho_0 - \rho_f) r(t) + \rho_f$ is a time-varying scaling function with $0 < \rho_f < \rho_0 \leq 1$ being some constants.

From (3), it is obvious that $\rho(t)$ has the following properties: (1) $\rho(t) = \rho_0, t = 0$; (2) $\rho(t) \in [\rho_f, \rho_0), \forall t > 0$; and (3) $\dot{\rho}(t)$, is known, bounded, and piece-wise continuous.

As $\rho(t)$ is non-monotonic with respect to t, and $\mathcal{P}(\rho)$ is strictly monotonic with respect to $\rho \in (0, 1)$, it results that $\mathcal{P}(\rho)$ is non-monotonic with respect to t.

Remark 1: In [19]–[22], the time-varying scaling function $\rho(t)$ must monotonically decrease over time, however, this strict monotonicity is not always suitable. For example, in the presence of periodic disturbances or highly fluctuating reference signals, it may be advantageous to expand the performance boundaries within certain time intervals. Therefore, non-monotonic time-varying scaling functions may be beneficial in some practical scenarios.

C. A Novel Nussbaum-type Function

A continuous function $N(\chi)$ is called a Nussbaum-type function if it satisfies the following properties [30]:

$$\begin{aligned} &\lim_{s \to \pm\infty} \sup \tfrac{1}{s} \textstyle\int_0^s N(\chi)\, d\chi = +\infty, \\ &\lim_{s \to \pm\infty} \inf \tfrac{1}{s} \textstyle\int_0^s N(\chi)\, d\chi = -\infty. \end{aligned} \tag{4}$$

$N(\chi)$ commonly selected as $\chi^2 \sin(\chi)$, $\chi^2 \cos(\chi)$, or $e^{\chi^2} \cos(\chi)$. However, analyzing the interactions of coexisting Nussbaum functions in a single inequality proves challenging, as elaborated in Remark 2. To this end, the following Nussbaum functions are introduced:

$$\begin{aligned} N_i(\chi) = &\, 2\chi \sinh\left(\chi^2\right) \cos\left(2^{i-1}\chi\right) \\ &- 2^{i-1}\left[\cosh\left(\chi^2\right) - 1\right] \sin\left(2^{i-1}\chi\right), \end{aligned} \tag{5}$$

where $i = 1, 2, \ldots, n$.

Theorem 1: For a smooth positive definite Lyapunov function $V(t)$ defined on $[0, T_f)$, and Nussbaum functions $N_i(\chi_i), i = 1, 2, \ldots, n$ defined in (5) with $\chi_i(t)$ being Nussbaum variables defined on $[0, T_f)$, if the following inequality holds for $t \in [0, T_f)$:

$$\mathcal{L}V(t) \leq -\sigma V(t) + \beta + \sum_{i=1}^{n} \left[b_i(\tau) N_i(\chi_i) + 1\right] \dot{\chi}_i, \tag{6}$$

where σ and β denote some positive constants, and $b_i(\tau)$ are non-zero time-varying functions, then $V(t)$, $\chi_i(t)$, and $\sum_{i=1}^{n} \left[b_i(t) N_i(\chi_i) + 1\right] \dot{\chi}_i$ are bounded in probability on $[0, T_f)$.

Proof: See Appendix.

Remark 2: In the existing works [21], [27]–[30] that employ the Nussbaum function to handle unknown control directions, the proof of inequality (6) is based on either a single Nussbaum function or multiple Nussbaum functions that have identical control direction. When considering inequalities involving multiple Nussbaum functions and different control directions, such as $\sum_{i=1}^{n} c_i \chi_i^2 \sin(\chi_i)$, where c_i represent the sign of the unknown directions $b_i(t)$ with $c_i = -1$ or $c_i = 1$, the establishment of the boundedness of χ_i remains a challenging issue. The difficulty arises because the unknown sign of $\sin(\chi_i)$ may cause terms in the inequality to potentially cancel each other out. To address this challenge, this paper introduces the novel Nussbaum functions (5) where each function is characterized by a distinct frequency, thereby overcoming the aforementioned obstacles. In addition, unlike [31]–[33], the multiple Nussbaum functions (5) can be directly applied to stochastic nonlinear systems, thus complementing the theoretical research in this area. Furthermore, the multiple Nussbaum functions (5) no longer rely on a priori knowledge of system parameters, thus offering more versatility.

D. Preliminaries

Definition 1 [17]: Consider the stochastic system (1) with $f = [f_1, f_2, \ldots, f_n]^T$ and $g = [g_1, g_2, \ldots, g_n]^T$. For any smooth Lyapunov function $V(x) > 0$, the differential operator $\mathcal{L}$ is defined as follows:

$$\mathcal{L}V(x) = \frac{\partial V}{\partial x} f(x) + \frac{1}{2} Tr\left\{g^T(x) \frac{\partial^2 V}{\partial x^2} g(x)\right\}, \tag{7}$$

where $Tr\{\cdot\}$ denotes the trace of the matrix.

Lemma 1 [10]: For functions $\Phi_1(\cdot), \Phi_2(\cdot) \in k_\infty$, and constants $\sigma, \beta > 0$, if the following conditions hold true:

$$\begin{aligned} &\Phi_1(\|x\|) \leq V(x) \leq \Phi_2(\|x\|), \\ &\mathcal{L}V(x) \leq -\sigma V(x) + \beta, \end{aligned} \tag{8}$$

then, the solution of system (1) is bounded in probability.

Lemma 2 [37]: For any $\wp > 0$ and $\Im \in \mathbb{R}$, one has

$$0 \leq |\Im| - \frac{2}{\pi} \Im \arctan\left(\frac{\Im}{\wp}\right) \leq \frac{2}{\pi} \wp. \tag{9}$$

Fuzzy logic systems (FLSs) will be introduced to approximate nonlinear functions.

A FLS can be expressed as:

$$Y(X) = \frac{\sum_{i=1}^{N} \psi_i \prod_{j=1}^{n} \kappa_{U_j^i}(X_j)}{\sum_{i=1}^{N} \left[\prod_{j=1}^{n} \kappa_{U_j^i}(X_j)\right]}, \tag{10}$$

where $\kappa_{U_j^i}$ are the membership functions, $\psi_i = \max_{Y \in R}\{\kappa_{A^i}(Y)\}$, and N is the number of IF-THEN rules, i.e., if X_1 is U_1^i and $\cdots$ and X_n is U_n^i, then Y is A^i. Let

$$h_i(X) = \frac{\prod_{j=1}^{n} \kappa_{U_j^i}(X_j)}{\sum_{i=1}^{N} \left[\prod_{j=1}^{n} \kappa_{U_j^i}(X_j)\right]}, \tag{11}$$

where $H = [h_1(X), h_2(X), \ldots, h_N(X)]^T$, and $\psi = [\psi_1, \ldots, \psi_N]^T$.

From (10) and (11), one has

$$Y(X) = \psi^T H(X). \tag{12}$$

Lemma 3 [33]: Given an unknown smooth function $F(X)$ defined on a compact set Ω, it is possible to introduce a FLS $\psi^T H(X)$ that approximates $F(X)$ while satisfying the following conditions:

$$\sup_{X\in\Omega} \left|F(X) - \psi^T H(X)\right| \le \varepsilon, \tag{13}$$

where ψ and $H(X)$ denote the ideal weight vector and the basis function vector, respectively, and $\varepsilon > 0$ denotes a constant.

Assumption 1 [30]: The reference signal $y_d(t)$ and its derivatives $\dot{y}_d(t)$ are known, continuous, and bounded.

Assumption 2 [32]: The time-varying control coefficients $b_i(t)$ have unknown lower and upper bounds, i.e., $0 < \underline{b}_i \le |b_i(t)| \le \bar{b}_i$.

III. Main Results

A. State Transformation

Define the tracking error of system (1) as $e(t) = x_1(t) - y_d(t)$. To ensure the prescribed performance $\mathcal{P}(-\underline{\varsigma}\rho(t)) < e(t) < \mathcal{P}(\bar{\varsigma}\rho(t))$ for $t \ge 0$, we introduce the following asymmetric barrier function:

$$s(t) = \frac{\hbar(t)}{(\underline{\varsigma} + \hbar(t))(\bar{\varsigma} - \hbar(t))}, \tag{14}$$

where $\upsilon(e) = e(t)/\sqrt{e(t)^2 + l^2}$, $\hbar(t) = \upsilon(e)/\rho(t)$, and $\underline{\varsigma}$ and $\bar{\varsigma}$ are positive constants.

From (14), it is obvious that $\hbar(t)$ has the following properties: (1) if $\hbar(0)$ satisfies $-\underline{\varsigma} < \hbar(0) < \bar{\varsigma}$, then $s(t) \to \pm\infty$ if and only if $\hbar(t) \to \underline{\varsigma}$ or $\hbar(t) \to \bar{\varsigma}$; and (2) if $\hbar(0)$ satisfies $-\underline{\varsigma} < \hbar(0) < \bar{\varsigma}$ and $s(t)$ is bounded for $t \ge 0$, then there exist two constants $\underline{\xi}$ and $\bar{\xi}$ such that $-\underline{\varsigma} < -\underline{\xi} < \hbar(0) < \bar{\xi} < \bar{\varsigma}$.

Then, we can deduce the derivative of (14) as

$$ds(t) = \iota_1(t) d\hbar(t), \tag{15}$$

where $\iota_1(t) = \left(\underline{\varsigma}\bar{\varsigma} + \hbar^2(t)\right) / \left((\underline{\varsigma} + \hbar(t))^2 (\bar{\varsigma} - \hbar(t))^2\right)$.

Note that

$$d\hbar(t) = \frac{\iota_2(t)}{\rho(t)} de(t) - \frac{d\rho(t)}{\rho^2(t)} \upsilon(e), \tag{16}$$

where $\iota_2(t) = l^2 / \left(\sqrt{(e^2(t) + l^2)}\left(e^2(t) + l^2\right)\right) > 0$.

Substituting (16) into (15) yields

$$ds(t) = \lambda_1(t)\left(dx_1(t) - \dot{y}_d(t)\right) + \lambda_2(t), \tag{17}$$

where $\lambda_1(t) = \iota_1(t)\iota_2(t)/\rho(t)$ and $\lambda_2(t) = -\iota_1(t) d\rho(t) \upsilon(e)/\rho^2(t)$.

Next, we prove that (14) ensures that $\mathcal{P}(-\underline{\varsigma}\rho(t)) < e(t) < \mathcal{P}(\bar{\varsigma}\rho(t))$ for $t \ge 0$.

Theorem 2: If the boundedness of $s(t)$ is ensured for $t \ge 0$, then for any initial condition $\hbar(0)$ satisfying $-\underline{\varsigma} < \hbar(0) < \bar{\varsigma}$, then $e(t)$ is bounded as $\mathcal{P}(-\underline{\varsigma}\rho(t)) < e(t) < \mathcal{P}(\bar{\varsigma}\rho(t))$ for $t \ge 0$.

Proof: Considering $-\underline{\varsigma} < \hbar(0) < \bar{\varsigma}$, it can be readily verified that $s(t)$ is well-defined at $t = 0$. Moreover, if the control system being developed ensures that $s(t)$ remains bounded for $t \ge 0$, it follows from the properties of the barrier function that $s(t)$ will not approach the boundary values $\underline{\varsigma}$ and $\bar{\varsigma}$. In other words, $-\underline{\varsigma} < \hbar(t) < \bar{\varsigma}$ for $t \ge 0$. By considering the definition of $\hbar(t)$ as in (14), we can establish that $-\underline{\varsigma}\rho(t) < \upsilon(e) < \bar{\varsigma}\rho(t)$. Given that $\mathcal{P}(\rho)$ is strictly monotonic with respect to $\rho(t)$, it follows that $\mathcal{P}(-\underline{\varsigma}\rho(t)) < \mathcal{P}(\upsilon(e)) < \mathcal{P}(\bar{\varsigma}\rho(t))$. Referring to the expressions of $\mathcal{P}(\rho)$ and $\upsilon(e)$ presented in equations (3) and (14) respectively, it can be observed that $e(t) = l\upsilon(e)/\sqrt{1 - \upsilon^2(e)} = \mathcal{P}(\upsilon(e))$. Consequently, the inequality $\mathcal{P}(-\underline{\varsigma}\rho(t)) < \mathcal{P}(\upsilon(e)) < \mathcal{P}(\bar{\varsigma}\rho(t))$ can be rewritten as $\mathcal{P}(-\underline{\varsigma}\rho(t)) < e(t) < \mathcal{P}(\bar{\varsigma}\rho(t))$, where $\mathcal{P}(-\underline{\varsigma}\rho(t)) = -l\underline{\varsigma}\rho(t)/\sqrt{1 - (\underline{\varsigma}\rho(t))^2}$ and $\mathcal{P}(\bar{\varsigma}\rho(t)) = l\bar{\varsigma}\rho(t)/\sqrt{1 - (\bar{\varsigma}\rho(t))^2}$. At this stage, we have completed the proof of Theorem 2.

The aforementioned analysis reveals that, by using the barrier function (14), ensuring that the tracking error satisfies the prescribed performance $\mathcal{P}(-\underline{\varsigma}\rho(t)) < e(t) < \mathcal{P}(\bar{\varsigma}\rho(t))$ for $t \ge 0$ simplifies to ensuring the boundedness of $s(t)$.

Remark 3: In this remark, we analyze four different performance behaviors of the proposed non-monotonic prescribed performance function for different values of ρ_0, $\underline{\varsigma}$, and $\bar{\varsigma}$.

(1) If $\rho_0 = \underline{\varsigma} = \bar{\varsigma} = 1$, then $\mathcal{P}(-\underline{\varsigma}\rho(0)) = -\infty$ and $\mathcal{P}(\bar{\varsigma}\rho(0)) = +\infty$, i.e., $-\infty < e(0) < +\infty$. This indicates that the initial error is not constrained by a lower and an upper bounds and the initial feasibility conditions are completely eliminated. Therefore, when the initial error changes, there is no longer a need to evaluate the feasibility condition or redesign the prescribed performance function.

(2) If $\rho_0 = \bar{\varsigma} = 1$ and $0 < \underline{\varsigma} < 1$, then $\mathcal{P}(-\underline{\varsigma}\rho(0)) = -\underline{\Lambda}$ with $\underline{\Lambda} > 0$ being a bounded constant, i.e., $-\underline{\Lambda} < e(0) < +\infty$. This indicates that the initial error is constrained by a lower bound but not by an upper bound. In other words, an asymmetric constraint of upward extrusion is formed, thus adjustments have to be made to the output overshoot when the initial error direction is positive.

(3) If $\rho_0 = \underline{\varsigma} = 1$ and $0 < \bar{\varsigma} < 1$, then $\mathcal{P}(\bar{\varsigma}\rho(0)) = \bar{\Lambda}$ with $\bar{\Lambda} > 0$ being a bounded constant, i.e., $-\infty < e(0) < \bar{\Lambda}$. This indicates that the initial error is constrained by an upper bound but not by a lower bound. In other words, an asymmetric constraint of downward extrusion is formed, thus adjustments have to be made to the output overshoot when the initial error direction is negative.

(4) If $0 < \underline{\varsigma}\rho_0 < 1$ and $0 < \bar{\varsigma}\rho_0 < 1$, then $\mathcal{P}(-\underline{\varsigma}\rho(0)) = -\underline{\Lambda}$ and $\mathcal{P}(\bar{\varsigma}\rho(0)) = \bar{\Lambda}$, i.e., $-\underline{\Lambda} < e(0) < \bar{\Lambda}$. In this case, the initial error is constrained by both a lower and an upper bound. An asymmetric constraint can be introduced at this stage, as long as the initial error satisfies the feasibility condition. However, if the initial error changes and violates the feasibility condition, the prescribed performance function needs to be redesigned.

Remark 4: Based on the discussions above, by varying the values of ρ_0, $\underline{\varsigma}$, and $\bar{\varsigma}$, the non-monotonic prescribed performance function designed in this paper can achieve similar constrained/unconstrained initial values, symmetric/asymmetric constraints as seen in references [21], [27]–[30]. Moreover, the overall performance boundary monotonicity can be modified by adjusting the monotonicity of $r(t)$. In other words, when a non-monotonic $r(t)$ is employed, the prescribed performance function will also display non-monotonic behavior. Conversely, opting for a monotonic $r(t)$ will yield a prescribed performance function that is also monotonic. Furthermore, the form of $r(t)$ will also determine whether the prescribed performance function has an adjustable settling time. For example, if $r(t)$ is chosen as $r(t) = \exp(-at)\cos^2(t)$, the prescribed function cannot specify a settling time, whereas when $r(t) = \begin{cases} \left(\frac{T-t}{T}\right)^{a+1}\cos^2(t), 0 \le t < T \\ 0, t \ge T \end{cases}$, the settling time can be precisely set by adjusting the value of T. It is important to note that the form of $r(t)$ is not unique. Here we have only listed some commonly used forms, but other forms of $r(t)$ with similar properties can also be developed and utilized.

In summary, the non-monotonic prescribed performance function designed in this paper provides a more convenient approach to meet practical control requirements. Practitioners only need to adjust ρ_0, $\underline{\varsigma}$, $\bar{\varsigma}$, and $r(t)$ to achieve different performance behaviors.

B. Adaptive Fuzzy Control Design

Design the following error system:

$$v_i(t) = \begin{cases} s(t), i = 1, \\ x_i(t) - \bar{\alpha}_{i-1}(t), i = 2, 3, \ldots n, \end{cases} \tag{18}$$

where $\bar{\alpha}_{i-1}(t), i = 2, 3, \ldots n$, denote the output of the Levant filter [48]:

$$\begin{cases} \dot{\varphi}_{i,1} = \vartheta_{i,1}, \\ \vartheta_{i,1} = -r_{i,1}|\varphi_{i,1} - \alpha_{i-1}|^{\frac{1}{2}}\operatorname{sign}(\varphi_{i,1} - \alpha_{i-1}) \\ \qquad + \varphi_{i,2}, \\ \dot{\varphi}_{i,2} = -r_{i,2}\operatorname{sign}(\varphi_{i,2} - \dot{\varphi}_{i,1}), \end{cases} \tag{19}$$

where $\bar{\alpha}_{i-1} = \varphi_{i,1}$ and $\dot{\bar{\alpha}}_{i-1} = \vartheta_{i,1}$. $r_{i,1}, r_{i,2} > 0$ are design parameters. According to [48], $|\bar{\alpha}_{i-1} - \alpha_{i-1}| \le o_i$ with $o_i, i = 1, 2, \ldots, n-1$ being some positive constants.

Remark 5: This paper uses a single-parameter estimation method to reduce the computational burden of adaptive parameters. In preparation for controller design, we predefine the following symbols: $\eta = \max\{\eta_i\}$, $\Theta = \max\{\Theta_i\}$, where $i = 1, 2, \ldots, n$, $\tilde{\eta} = \eta - \hat{\eta}$ represents the estimation error relative to the ideal value η and its estimated value $\hat{\eta}$, and $\tilde{\Theta} = \Theta - \hat{\Theta}$ denote the estimation error relative to the ideal value Θ and its estimated value $\hat{\Theta}$.

Step 1: The Lyapunov function is defined as

$$V_1 = \frac{1}{4}v_1^4 + \frac{1}{2\gamma}\tilde{\Theta}^T\tilde{\Theta} + \frac{1}{2\mu}\tilde{\eta}^T\tilde{\eta}, \tag{20}$$

where $\gamma, \mu > 0$ denote design parameters.

According to Definition 1, one has

$$\begin{aligned} \mathcal{L}V_1 \le{}& \lambda_1 v_1^3(b_1\alpha_1 + b_1 v_2 + b_1 o_1 + f_1 - \dot{y}_d) \\ &+ \lambda_2 v_1^3 - \tfrac{1}{\gamma}\tilde{\Theta}\dot{\hat{\Theta}} - \tfrac{1}{\mu}\tilde{\eta}\dot{\hat{\eta}} + \tfrac{3}{2}\lambda_1^2 v_1^2 Tr\left\{g_1^T g_1\right\}. \end{aligned} \tag{21}$$

Based on Young's inequality, one has

$$\begin{aligned} \tfrac{3}{2}\lambda_1^2 v_1^2 Tr\left\{g_1^T g_1\right\} &\le \tfrac{9}{8}\lambda_1^4 v_1^4\|g_1\|^4 + \tfrac{1}{2}, \\ b_1\lambda_1 v_1^3 v_2 &\le \tfrac{3}{4}\lambda_1^{\frac{4}{3}} v_1^4 + \tfrac{1}{4}\bar{b}_1^4 v_2^4, \\ b_1 o_1 \lambda_1 v_1^3 &\le \tfrac{3}{4}\lambda_1^{\frac{4}{3}} v_1^4 + \tfrac{1}{4}\bar{b}_1^4 o_1^4. \end{aligned} \tag{22}$$

Substituting (22) into (21) yields

$$\begin{aligned} \mathcal{L}V_1 \le{}& v_1^3\left[b_1\lambda_1\alpha_1 - \lambda_1\dot{y}_d + \lambda_2 + F_1(X_1) + \tfrac{3}{2}\lambda_1^{\frac{4}{3}}v_1\right] \\ &+ \tfrac{1}{4}\bar{b}_1^4 v_2^4 + \tfrac{1}{4}\bar{b}_1^4 o_1^4 + \tfrac{1}{2} - \tfrac{1}{\gamma}\tilde{\Theta}\dot{\hat{\Theta}} - \tfrac{1}{\mu}\tilde{\eta}\dot{\hat{\eta}}, \end{aligned} \tag{23}$$

where the unknown function is represented as $F_1(X_1) = \lambda_1 f_1 + (9/8)\lambda_1^4 v_1\|g_1\|^4$ and can be approximated using FLS, that is, $F_1(X_1) = \psi_1^T H_1(X_1) + \varepsilon_1(X_1)$. We assume that the FLS approximation error satisfies the condition $|\varepsilon_1(X_1)| \le \bar{\varepsilon}_1$, where $\bar{\varepsilon}_1 > 0$, and $X_1 = \left[\bar{x}_n^T, v_1, \rho\right]^T$.

According to Lemma 2 and Young's inequality, one has

$$\begin{aligned} v_1^3 F_1 &\le \tfrac{v_1^6}{2a_1^2}\Theta_1\|H_1\|^2 + \tfrac{1}{2}a_1^2 + \left|v_1^3\right||\varepsilon_1| \\ &\le \tfrac{v_1^6}{2a_1^2}\Theta\|H_1\|^2 + \tfrac{1}{2}a_1^2 + \left|v_1^3\right|\bar{\varepsilon}_1, \\ \left|v_1^3\right|\bar{\varepsilon}_1 &= \left|v_1^3\right|\eta_1 \le \tfrac{2}{\pi}v_1^3\eta\arctan\left(\tfrac{v_1^3}{\tau_1}\right) + \tfrac{2}{\pi}\tau_1\eta, \end{aligned} \tag{24}$$

where a_1, $\tau_1 > 0$ are design parameters, $\Theta_1 = \|\psi_1\|^2$, and $\eta_1 = \bar{\varepsilon}_1$.

Substituting (24) into (23) yields

$$\begin{aligned} \mathcal{L}V_1 \le{}& v_1^3\Big[b_1\lambda_1\alpha_1 - \lambda_1\dot{y}_d + \lambda_2 + \tfrac{3}{2}\lambda_1^{\frac{4}{3}}v_1 \\ &+ \tfrac{v_1^3}{2a_1^2}\hat{\Theta}\|H_1\|^2 + \tfrac{2}{\pi}\hat{\eta}\arctan\left(\tfrac{v_1^3}{\tau_1}\right)\Big] + \tfrac{2}{\pi}\tau_1\eta \\ &+ \tfrac{1}{4}\bar{b}_1^4 o_1^4 + \tfrac{1+a_1^2}{2} - \tfrac{1}{\gamma}\tilde{\Theta}\left(\tfrac{\gamma v_1^6}{2a_1^2}\|H_1\|^2 - \dot{\hat{\Theta}}\right) \\ &- \tfrac{1}{\mu}\tilde{\eta}\left[\tfrac{2\mu}{\pi}v_1^3\arctan\left(\tfrac{\lambda_1 v_1^3}{\tau_1}\right) - \dot{\hat{\eta}}\right] + \tfrac{1}{4}\bar{b}_1^4 v_2^4. \end{aligned} \tag{25}$$

Design the virtual control law α_1 using the Nussbaum function for the first subsystem as follows:

$$\begin{cases} \alpha_1 = \frac{N_1(\chi_1)}{\lambda_1}\Xi_1, \\ \Xi_1 = k_1 v_1 - \lambda_1\dot{y}_d + \lambda_2 + \frac{3}{2}\lambda_1^{\frac{4}{3}}v_1 \\ \qquad + \frac{v_1^3}{2a_1^2}\hat{\Theta}\|H_1\|^2 + \frac{2}{\pi}\hat{\eta}\arctan\left(\frac{v_1^3}{\tau_1}\right), \\ \dot{\chi}_1 = v_1^3\Xi_1, \end{cases} \tag{26}$$

where $k_1 > 0$ is a design parameter.

Substituting (26) into (25) yields

$$\begin{aligned} \mathcal{L}V_1 \le{}& -k_1 v_1^4 - \tfrac{1}{\gamma}\tilde{\Theta}\left(\tfrac{\gamma v_1^6}{2a_1^2}\|H_1\|^2 - \dot{\hat{\Theta}}\right) + \tfrac{2}{\pi}\tau_1\eta \\ &- \tfrac{1}{\mu}\tilde{\eta}\left[\tfrac{2\mu}{\pi}v_1^3\arctan\left(\tfrac{v_1^3}{\tau_1}\right) - \dot{\hat{\eta}}\right] + \tfrac{1+a_1^2}{2} \\ &+ \tfrac{1}{4}\bar{b}_1^4 o_1^4 + \tfrac{1}{4}\bar{b}_1^4 v_2^4 + \left[b_1 N_1(\chi_1) + 1\right]\dot{\chi}_1. \end{aligned} \tag{27}$$

Step $i\,(i = 2, \ldots, n-1)$: Considering the similarity between the derivation process of the *i*-th subsystems and Step 1, only a few essential expressions are presented here. The Nussbaum functions are utilized to design virtual control laws α_i in the following manner:

$$\begin{cases} \alpha_i = N_i(\chi_i)\Xi_i, \\ \Xi_i = k_i v_i - \dot{\bar{\alpha}}_{i-1} + \frac{3}{2}v_i \\ \qquad + \frac{v_i^3}{2a_i^2}\hat{\Theta}\|H_i\|^2 + \frac{2}{\pi}\hat{\eta}\arctan\left(\frac{v_i^3}{\tau_i}\right), \\ \dot{\chi}_i = v_i^3\Xi_i, \end{cases} \tag{28}$$

where a_{i1}, k_i, $\tau_i \in \mathbb{R}^+$ are design constants, $\Theta_i = \|\psi_i\|^2$, and $\eta_i = \bar{\varepsilon}_i$. Moreover, similar to Step 1, we define $F_i(X_i) = f_i + (9/8)\, v_i \|g_i\|^4$ and then employ FLSs to approximate $F_i(X_i)$, i.e., $F_i(X_i) = \psi_i^T H_i(X_i) + \varepsilon_i(X_i)$. We assume that the FLS approximation error satisfies the condition $|\varepsilon_i(X_i)| \le \bar{\varepsilon}_i$, where $\bar{\varepsilon}_i \in \mathbb{R}^+$, $X_i = \left[\bar{x}_i^T, v_i\right]^T$.

The Lyapunov function is defined as

$$V_i = V_{i-1} + \frac{1}{4} v_i^4, \tag{29}$$

From (28)–(29), one has

$$\begin{aligned} \mathcal{L}V_i \le & -\sum_{j=1}^{i} k_j v_j^4 + \sum_{j=1}^{i} \tfrac{1+a_j^2}{2} + \sum_{j=1}^{i} \tfrac{2}{\pi}\tau_j \eta \\ & + \sum_{j=1}^{i} \left[b_j N_j(\chi_j) + 1\right] \dot{\chi}_j + \sum_{j=1}^{i} \tfrac{1}{4}\bar{b}_j^4 v_{j+1}^4 \\ & + \sum_{j=1}^{i} \tfrac{1}{4}\bar{b}_j^4 o_j^4 - \tfrac{1}{\gamma}\tilde{\Theta}\left(\sum_{j=1}^{i} \tfrac{\gamma v_j^6}{2a_j^2}\|H_j\|^2 - \dot{\hat{\Theta}}\right) \\ & - \tfrac{1}{\mu}\tilde{\eta}\left[\sum_{j=1}^{i} \tfrac{2\mu}{\pi} v_j^3 \arctan\left(\tfrac{v_j^3}{\tau_j}\right) - \dot{\hat{\eta}}\right]. \end{aligned} \tag{30}$$

Step n: The Lyapunov function is defined as

$$V_n = V_{n-1} + \frac{1}{4} v_n^4. \tag{31}$$

The following is obtained from (30) and (31):

$$\begin{aligned} \mathcal{L}V_n \le & -\sum_{j=1}^{n-1} k_j v_j^4 - \tfrac{1}{\gamma}\tilde{\Theta}\left(\sum_{j=1}^{n-1} \tfrac{\gamma v_j^6}{2a_j^2}\|H_j\|^2 - \dot{\hat{\Theta}}\right) \\ & - \tfrac{1}{\mu}\tilde{\eta}\left[\sum_{j=1}^{n-1} \tfrac{2\mu}{\pi} v_j^3 \arctan\left(\tfrac{v_j^3}{\tau_j}\right) - \dot{\hat{\eta}}\right] \\ & + \tfrac{1}{2} + \sum_{j=1}^{n-1} \tfrac{1+a_j^2}{2} + \sum_{j=1}^{n-1} \tfrac{2}{\pi}\tau_j \eta + \sum_{j=1}^{n} \tfrac{1}{4}\bar{b}_j^4 o_j^4 \\ & + \sum_{j=1}^{n-1} \left[b_j N_j(\chi_j) + 1\right] \dot{\chi}_j + \sum_{j=1}^{n-1} \tfrac{1}{4}\bar{b}_j^4 v_{j+1}^4 \\ & + v_n^3 \left[b_n u - \dot{\alpha}_{n-1} + \tfrac{3}{4} v_n + F_n(X_n)\right], \end{aligned} \tag{32}$$

where $F_n(X_n) = f_n + \frac{9}{8} v_n \|g_n\|^4$ and can be approximated using FLS, that is, $F_n(X_n) = \psi_n^T H_n(X_n) + \varepsilon_n(X_n)$. We assume that the FLS approximation error satisfies the condition $|\varepsilon_n(X_n)| \le \bar{\varepsilon}_n$, where $\bar{\varepsilon}_n \in \mathbb{R}^+$, $X_n = \left[\bar{x}_n^T, v_n\right]^T$.

By applying Young's inequality and Lemma 2, the following inequalities apply:

$$\begin{aligned} v_n^3 F_n \le & \tfrac{v_n^6}{2a_n^2}\Theta_n \|H_n\|^2 + \tfrac{1}{2}a_n^2 + \left|v_n^3\right| |\varepsilon_n| \\ \le & \tfrac{v_n^6}{2a_n^2}\Theta \|H_n\|^2 + \tfrac{1}{2}a_n^2 + \left|v_n^3\right| \bar{\varepsilon}_n, \\ \left|v_n^3\right| \bar{\varepsilon}_n = & \left|v_n^3\right| \eta_n \le \tfrac{2}{\pi} v_n^3 \eta \arctan\left(\tfrac{v_n^3}{\tau_n}\right) + \tfrac{2}{\pi}\tau_n \eta, \end{aligned} \tag{33}$$

where a_n, $\tau_n \in \mathbb{R}^+$ are design constants, $\Theta_n = \|\psi_n\|^2$, and $\eta_n = \bar{\varepsilon}_n$.

Substituting (33) into (32) yields

$$\begin{aligned} \mathcal{L}V_n \le & -\sum_{j=1}^{n-1} k_j v_j^4 - \tfrac{1}{\gamma}\tilde{\Theta}\left(\sum_{j=1}^{n} \tfrac{\gamma v_j^6}{2a_j^2}\|H_j\|^2 - \dot{\hat{\Theta}}\right) \\ & - \tfrac{1}{\mu}\tilde{\eta}\left[\sum_{j=1}^{n} \tfrac{2\mu}{\pi} v_j^3 \arctan\left(\tfrac{v_j^3}{\tau_j}\right) - \dot{\hat{\eta}}\right] \\ & + \sum_{j=1}^{n} \tfrac{1+a_j^2}{2} + \sum_{j=1}^{n} \tfrac{2}{\pi}\tau_j \eta + \sum_{j=1}^{n} \tfrac{1}{4}\bar{b}_j^4 o_j^4 \\ & + \sum_{j=1}^{n-1} \left[b_j N_j(\chi_j) + 1\right] \dot{\chi}_j + \sum_{j=1}^{n-1} \tfrac{1}{4}\bar{b}_j^4 v_{j+1}^4 \\ & + v_n^3 \left[-b_n \alpha_n - \dot{\alpha}_{n-1} + \tfrac{3}{4} v_n + F_n(X_n)\right] \\ & + b_n v_n^3 (u + \alpha_n). \end{aligned} \tag{34}$$

Design α_n, $\dot{\hat{\Theta}}$, and $\dot{\hat{\eta}}$ with support from the Nussbaum-type function for the *n*-th subsystem as follows:

$$\begin{cases} \alpha_n = -N_n(\chi_n)\, \Xi_n, \\ \Xi_n = k_n v_n - \dot{\alpha}_{n-1} + \tfrac{3}{4} v_n + \tfrac{3}{4} v_n \\ \qquad + \tfrac{v_n^3}{2a_n^2}\hat{\Theta}\|H_n\|^2 - \tfrac{2}{\pi}\hat{\eta} \arctan\left(\tfrac{v_n^3}{\tau_n}\right), \\ \dot{\chi}_n = v_n^3 \Xi_n, \\ \dot{\hat{\Theta}} = \sum_{j=1}^{n} \tfrac{\gamma v_j^6}{2a_j^2} \|H_j\|^2 - p_\Theta \hat{\Theta}, \\ \dot{\hat{\eta}} = \sum_{j=1}^{n} \tfrac{2\mu}{\pi} v_j^3 \arctan\left(\tfrac{v_j^3}{\tau_j}\right) - p_\eta \hat{\eta}, \end{cases} \tag{35}$$

where $p_\Theta, p_\eta \in \mathbb{R}^+$ are design constants.

Substituting (35) into (34) yields

$$\begin{aligned} \mathcal{L}V_n \le & -\sum_{j=1}^{n} k_j v_j^4 + \sum_{j=1}^{n} \tfrac{2+a_j^2}{4} + \sum_{j=1}^{n} \tfrac{2}{\pi}\tau_j \eta \\ & + \sum_{j=1}^{n} \left[b_j N_j(\chi_j) + 1\right] \dot{\chi}_j + \sum_{j=1}^{n} \tfrac{1}{4}\bar{b}_j^4 o_j^4 \\ & + \sum_{j=1}^{n-1} \tfrac{1}{4}\bar{b}_j^4 v_{j+1}^4 + \tfrac{p_\Theta}{\gamma}\tilde{\Theta}\hat{\Theta} + \tfrac{p_\eta}{\mu}\tilde{\eta}\hat{\eta} \\ & + b_n v_n^3 (u + \alpha_n) + \tfrac{3}{4} v_n^4. \end{aligned} \tag{36}$$

Remark 6: To facilitate the application of this research in various engineering contexts based on specific requirements, α_n is predetermined (instead of directly obtaining u) to allow for the integration of techniques such as event trigger, hysteresis quantization, and control inputs related to actuator failure.

Next, a novel non-conservative ETM is introduced as

$$\begin{cases} \omega(t) = -\tfrac{2\alpha_n}{\pi(1-\Im)} \arctan\left(\tfrac{v_n^3 \alpha_n}{\wp}\right), \\ u(t) = \omega\left(t^k\right), \forall t \in \left[t^k, t^{k+1}\right), \delta(t) = u(t) - \omega(t), \\ t^{k+1} = \begin{cases} \inf\left\{t > t^k \,||\delta(t)| \ge \Im|\omega(t)| + m_1 e^{-m_2 t}\right\}, \\ \text{if } |\omega(t)| < D, \\ \inf\left\{t > t^k \,||\delta(t)| \ge n\right\}, \\ \text{if } |\omega(t)| \ge D, \end{cases} \end{cases} \tag{37}$$

where $D, n, m_1, m_2, \wp > 0$, $0 < \Im < 1$ are design parameters, $\delta(t)$ denotes the measurement error, and t^k denotes the update time. The working principle of ETM is as follows: Within a specific interval $\left[t^k, t^{k+1}\right]$, where $u\left(t^k\right)$ acts as the control signal, upon triggering of ETM, an instantaneous transition occurs from t^k to t^{k+1}, concurrently resulting in the transformation of $u\left(t^k\right)$into $u\left(t^{k+1}\right)$.

Remark 7: In the previous study [34], the ETM is designed as $t^{k+1} = \inf\left\{t > t^k \left|\left|\delta(t)\right| \geq \Im\left|u(t)\right| + m_1\right.\right\}$ or $t^{k+1} = \inf\left\{t > t^k \left|\left|\delta(t)\right| \geq m_1\right.\right\}$ to determine the update instant. However, the controller proposed in [34] deemed conservative due to the inclusion of a robust term $\bar{m}_1 \tanh\left(\bar{m}_1\alpha_n/\wp\right)$. Because the parameters $\wp$, m_1, and $\bar{m}_1$ had to be satisfy the specific inequality constraint $\bar{m}_1 > m_1/\left(1-\delta\right)$ or $\bar{m}_1 > m_1$, aimed at compensating for the constant error m_1. In our paper, the novel ETM (37) is proposed, which effectively addresses constant measurement errors by integrating an arctan function, thereby overcoming the limitations of $\bar{m}_1 > m_1/\left(1-\delta\right)$ or $\bar{m}_1 > m_1$.

Remark 8: The ETM (37) is a switching threshold form that can adjust the balance between a fixed threshold and a relative threshold by tuning the parameter D. Specifically, when the control signal amplitude is small, a larger value of D can be set to prioritize the relative threshold strategy for precise control. Conversely, when the control signal amplitude is large, a smaller value of D can be set to prioritize the fixed threshold strategy for preventing step signal impact.

C. Stability Analysis

Theorem 3: For system (1) with the virtual control and adaptive laws (26), (28), and (35), as well as the ETM (37) under Assumptions 1 and 2, the proposed control scheme ensures all signals of system (1) are bounded in probability; and (2) the tracking error always evolve within predefined boundaries, expressed as $\mathcal{P}\left(-\underline{\varsigma}\rho(t)\right) < e(t) < \mathcal{P}\left(\bar{\varsigma}\rho(t)\right)$.

Proof: From (37) and $v_n^3\omega \leq 0$, one has

$$v_n^3\delta \leq -\Im v_n^3\omega + \tfrac{3}{4}v_n^4 + \tfrac{1}{4}m_1^4. \tag{38}$$

According to Lemma 2, one has

$$\left(1-\Im\right)v_n^3\omega + v_n^3\alpha_n \leq \tfrac{2}{\pi}\wp. \tag{39}$$

The Lyapunov function is defined as

$$V = \sum_{i=1}^{n}\frac{1}{4}v_i^4 + \frac{1}{2\gamma}\tilde{\Theta}^T\tilde{\Theta} + \frac{1}{2\mu}\tilde{\eta}^T\tilde{\eta}. \tag{40}$$

Based on Young's inequality, one has

$$\begin{aligned} \tfrac{p_\Theta}{\gamma}\tilde{\Theta}\hat{\Theta} &\leq -\tfrac{p_\Theta}{2\gamma}\tilde{\Theta}^2 + \tfrac{p_\Theta}{2\gamma}\Theta^2, \\ \tfrac{p_\eta}{\mu}\tilde{\eta}\hat{\eta} &\leq -\tfrac{p_\eta}{2\mu}\tilde{\eta}^2 + \tfrac{p_\eta}{2\mu}\eta^2. \end{aligned} \tag{41}$$

Combining (38)–(41) yields

$$\begin{aligned} \mathcal{L}V \leq & -\sum_{i=1}^{n}k_iv_i^4 - \tfrac{p_\Theta}{2\gamma}\tilde{\Theta}^2 - \tfrac{p_\eta}{2\mu}\tilde{\eta}^2 + \sum_{i=1}^{n}\tfrac{2+a_i^2}{4} \\ & + \sum_{i=1}^{n}\tfrac{2}{\pi}\tau_j\eta + \sum_{i=1}^{n}\tfrac{1}{4}\bar{b}_i^4o_i^4 + \tfrac{p_\Theta}{2\gamma}\Theta^2 + \tfrac{p_\eta}{2\mu}\eta^2 \\ & + \tfrac{2}{\pi}\bar{b}_n\wp + \tfrac{1}{4}\bar{b}_n^4m_1^4 + \sum_{i=1}^{n-1}\tfrac{1}{4}\bar{b}_i^4v_{i+1}^4 \\ & + \sum_{i=1}^{n}\left[b_iN_i\left(\chi_i\right)+1\right]\dot{\chi}_i. \end{aligned} \tag{42}$$

From (42), there is

$$\mathcal{L}V \leq -\sigma V + \beta + \sum_{i=1}^{n}\left[b_iN_i\left(\chi_i\right)+1\right]\dot{\chi}_i + \sum_{i=2}^{n}\frac{1}{4}\bar{b}_{i-1}^4v_i^4, \tag{43}$$

where $\sigma = \min\left\{4k_i, p_\Theta, p_\eta\right\}$, $\beta = \sum\limits_{i=1}^{n}\frac{2+a_i^2}{4} + \sum\limits_{i=1}^{n}\frac{2}{\pi}\tau_i\eta + \sum\limits_{i=1}^{n}\frac{1}{4}\bar{b}_i^4o_i^4 + \frac{p_\Theta}{2\gamma}\Theta^2 + \frac{p_\eta}{2\mu}\eta^2 + \frac{2}{\pi}\bar{b}_i\wp + \frac{1}{4}\bar{b}_n^4m_1^4$.

It is important to note that we cannot directly apply Theorem 1 to assess the stability of (43) at this stage, as the boundedness of $\sum_{i=2}^{n}\bar{b}_{i-1}^4v_i^4/4$ is unknown. Therefore, we must first ensure the boundedness of $\sum_{i=2}^{n}\bar{b}_{i-1}^4v_i^4/4$.

From the derivation process of *step n*, we can observe that *step n* does not contain the term $\bar{b}_n^4v_{n+1}^4/4$. In other words, if we analyze *step n* independently, disregarding the preceding $(n-1)$ steps, Theorem 1 can be directly applied. Therefore, we can ensure the boundedness of all variables when analyzing *step n* independently. Thereafter, we employ Theorem 1 in a reverse manner $(n-1)$ times, ensuring the boundedness of $\bar{b}_i^4v_{i+1}^4/4$, $i = 1, 2, \ldots, n-1$. Consequently, the boundedness of $\sum_{i=2}^{n}\bar{b}_{i-1}^4v_i^4/4$ can be ensured. At this point, we can get $\left|\sum_{i=2}^{n}\bar{b}_{i-1}^4v_i^4/4\right| \leq \mho$ with $\mho > 0$ being a constant. Then, (43) can be rewritten as

$$\mathcal{L}V \leq -\sigma V + \beta_1 + \sum_{i=1}^{n}\left[b_iN_i\left(\chi_i\right)+1\right]\dot{\chi}_i, \tag{44}$$

where $\beta = \sum\limits_{i=1}^{n}\frac{2+a_i^2}{4} + \sum\limits_{i=1}^{n}\frac{2}{\pi}\tau_i\eta + \sum\limits_{i=1}^{n}\frac{1}{4}\bar{b}_i^4o_i^4 + \frac{p_\Theta}{2\gamma}\Theta^2 + \frac{p_\eta}{2\mu}\eta^2 + \frac{2}{\pi}\bar{b}_i\wp + \frac{1}{4}\bar{b}_n^4m_1^4 + \mho$.

Based on Theorem 1 and Lemma 1, it can be concluded that, with appropriate choices of σ and β_1, the following variables are bounded in probability: $V(t)$, $\tilde{\Theta}$, $\tilde{\eta}$ v_i, $\chi_i(t)$, and $\sum_{i=1}^{n}\left[b_i(t)N_i(\chi_i)+1\right]\dot{\chi}_i$, $i = 1, 2, \ldots, n$. According to Assumption 1 and (18), s and $x_i, i = 2, \ldots, n$ are bounded in probability. After ensuring the boundedness of s, it can be observed from Theorem 2 that $\mathcal{P}\left(-\underline{\varsigma}\rho(t)\right) < e(t) < \mathcal{P}\left(\bar{\varsigma}\rho(t)\right)$ is guaranteed.

Next, it is important to mention that $\delta(t) = u(t) - \omega(t)$, $\forall t \in \left[t^k, t^{k+1}\right)$. Hence, one can obtain

$$\frac{d}{dt}\left|\delta\right| \leq \frac{d}{dt}\left(\delta \times \delta\right)^{\frac{1}{2}} = \operatorname{sign}(\delta)\dot{\delta} \leq \left|\dot{\omega}\right|. \tag{45}$$

Since $\dot{\omega}(t)$ is bounded, $\dot{\omega}(t)$ continuously connects to the bounded signals when $t \in \left[t^k, t^{k+1}\right)$. In other words, there exists a constant $\Upsilon \in \mathbb{R}^+$ such that $\left|\dot{\omega}(t)\right| \leq \Upsilon$, $t \in \left[t^k, t^{k+1}\right)$, leading to the conclusion that $\left|\delta(t)\right| \leq \Upsilon\left(t - t^{k+1}\right)$, $t \in \left[t^k, t^{k+1}\right)$. It should be noted that $\delta\left(t^k\right) = 0$ and $\lim\limits_{t\to t^{k+1}}\left|\delta(t)\right| \leq \Im\left|\omega\left(t^{k+1}\right)\right| + m_1e^{-m_2t^{k+1}}$; thus, one has

$$m_1e^{-m_2t^{k+1}} \leq \lim_{t\to t^{k+1}}\left|\delta\right| \leq \Upsilon\Delta t, \tag{46}$$

where $\Delta t = t^{k+1} - t^k$. Evidently, $\Delta t > 0$ can be easily deduced for any finite time interval. Additionally, $t^k \to \infty$ can be observed as $k \to \infty$, which can be verified by searching for a contradiction. Specifically, assuming $t^\infty = \lim\limits_{k\to\infty}t^k < \infty$ leads to the implication that $\lim\limits_{k\to\infty}\Delta t = 0$. In conjunction with (46), it is certain that $m_1e^{-m_2t^\infty} \to 0$, $t \to \infty$. Therefore, the occurrence of Zeno behavior can be ruled out.

At this stage, we have completed the proof of Theorem 3.

Remark 9: This remark will provide a summary for selecting and adjusting controller parameters.

(1) Increasing the control gains k_i, p_Θ, and p_η can result in a larger σ, thereby increasing the upper of $v_i, i = 1, \ldots, n$, and improving tracking precision. However, excessive control gains may lead to a sharp increase in control signals, even causing instability in the control system. Therefore, in practical applications, it is necessary to carefully design control gains according to the specific requirements.

(2) Increasing the filter gains $r_{i,1}$ and $r_{i,2}, i = 2, \ldots, n$ can lead to an improvement in the accuracy of the filtering process. However, excessively high filter gains may lead to high-frequency oscillations, thus affecting transient tracking performance. Therefore, it is necessary to strike a balance between filtering accuracy and transient performance when adjusting filter gains.

(3) Adjusting the parameters of the performance function has been discussed in Remark 3. It is important to note that the parameter a in the rate function affects both the convergence speed and monotonicity of the rate function $r(t)$. A smaller value of a results in slower convergence of the rate function but more pronounced non-monotonicity. The parameter l in the performance function is used to adjust steady-state accuracy. A larger value of l leads to higher steady-state accuracy but requires a larger control input.

(4) Adjusting the parameter D of ETM has been discussed in Remark 8. Additionally, n, m_1, and m_2 affect the triggering threshold, decreasing n, m_1, and m_2 can result in more frequent event triggering. Moreover, $\Im$ and $\wp$ influence the dynamic performance of ETM. Smaller values of $\Im$ and $\wp$ can improve the dynamic performance of ETM but simultaneously increase the deterministic time, thereby resulting in a large number of triggered events.

(5) Other control parameters, such as $a_i, i = 1, \ldots, n$, γ and μ are designed to address potential singularity issues during the approximation process. When singularities occur, decreasing a_i, γ and μ can circumvent these singularities, thereby preventing controller errors.

IV. Simulation Results

Example: Consider a mass-spring-damper system [33] as follows:

$$\begin{cases} dx_1 = [b_1(t)\, x_2]\, dt, \\ dx_2 = \left[b_2(t)\, u - \frac{1}{m} f(x_1, x_2)\right] dt + \frac{1}{m} g(x_1)\, d\omega, \\ y = x_1, \end{cases} \tag{47}$$

where $m = 1/3$, $f(x_1, x_2) = 2x_1^2 + x_1^3 \sin(x_1, x_2) + 0.2x_2^2 \cos x_2^2$, $g(x_1) = 0.6x_1$, $b_1(t) = 1 + 0.8\cos(0.2t)$, and $b_2(t) = -1 - 0.5\sin^2(t)$. The desired trajectory was selected as $y_d = 0.5\sin(t)$. The main control parameters were selected as $k_1 = 50$, $k_2 = 25$, $\ell_1 = 0.005$, $\ell_2 = 0.005$, $r_{21} = 30$, $r_{22} = 15$, $a_1 = 0.02$, $a_2 = 0.05$, $\gamma = 0.2$, $\mu = 0.5$, $p_\Theta = 1$, $p_\eta = 1$, $\tau_1 = 2$, $\tau_2 = 2$, $l = 1$, $a = 3$, $T = 3$, $\rho_f = 0.1$, $D = 5$, $n = 2$, $m_1 = 0.5$, $m_2 = 0.5$, $\wp = 0.05$, and $\Im = 0.05$. The membership functions of FLSs were employed as $\kappa_{U_j^i} = e^{\left(X_j^i + 5 - i\right)/16}$ with $i = 1, 2, 3, 4, 5, 6$ and $j = 1, 2, 3$.

Additionally, the initial conditions are selected as $x_1 = 0.3$, $x_2 = 0$, $\chi_1(0) = 0$, $\chi_2(0) = -1$, $\Theta(0) = 0$, $\eta(0) = 0$, $\varphi_{2,1}(0) = 0$, and $\varphi_{2,2}(0) = 0$. We considered the following cases:

Case 1. Set $\rho_0 = \underline{\varsigma} = \bar{\varsigma} = 1$, and compare the performance behaviors with $x_1(0) = 0.3$ and $x_1(0) = -0.3$.

Case 2. Set $x_1(0) = 0.3$, $\rho_0 = \bar{\varsigma} = 1$, and compare the performance behaviors with $\underline{\varsigma} = 1$ and $\underline{\varsigma} = 0.6$.

Case 3. Set $x_1(0) = -0.3$, $\rho_0 = \underline{\varsigma} = 1$, and compare the performance behaviors with $\bar{\varsigma} = 1$ and $\bar{\varsigma} = 0.6$.

Case 4. Set $x_1(0) = 0.3$, and compare the performance behaviors with $\rho_0 = \underline{\varsigma} = \bar{\varsigma} = 1$ and $\rho_0 = 1, \underline{\varsigma} = 0.5, \bar{\varsigma} = 0.8$.

Case 5. Set $x_1(0) = 0.3$, $\rho_0 = \underline{\varsigma} = \bar{\varsigma} = 1$, consider constraining the control input to operate at only 20 percent effectiveness within $t \in [2, 2.5]$, and compare the performance behaviors between the unconstrained and constrained input.

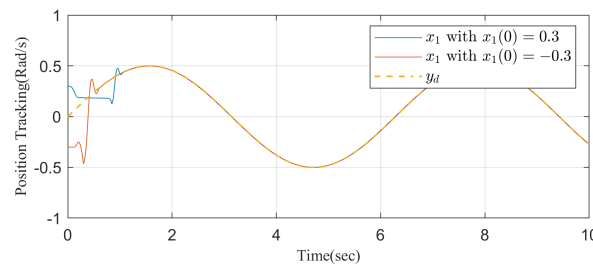

Fig. 1. Tracking trajectory with Case 1.

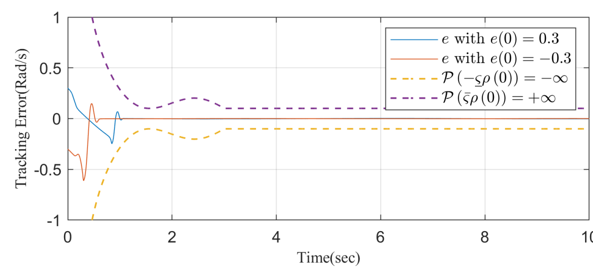

Fig. 2. Tracking error with Case 1.

Figs. 1 and 2 illustrate the performance behaviors achieved by setting parameters $\rho_0 = \underline{\varsigma} = \bar{\varsigma} = 1$ to remove upper and lower bounds on the initial value $x_1(0)$ (Case 1). From these two figures, it can be observed that with unconstrained initial boundaries, it is possible to autonomously adjust $x_1(0)$ without the need for redesigning the performance function, thus removing the initial value feasibility condition mentioned in references [41] and [42].

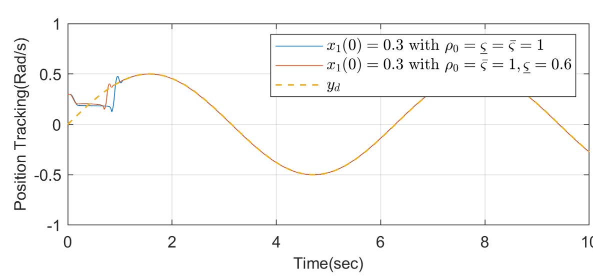

Fig. 3. Tracking trajectory with Case 2.

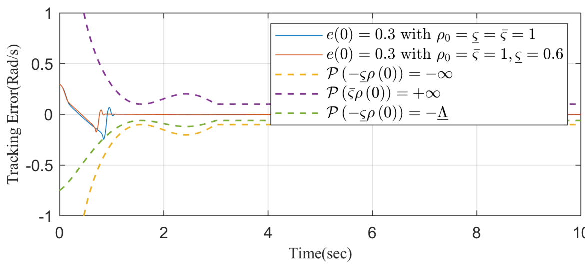

Fig. 4. Tracking error with Case 2.

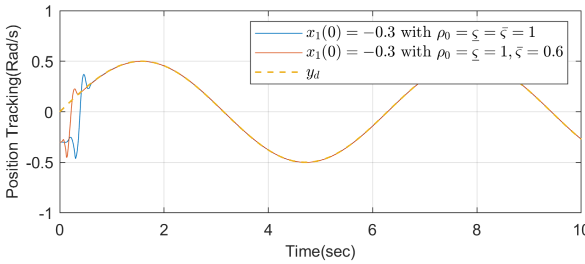

Fig. 5. Tracking trajectory with Case 3.

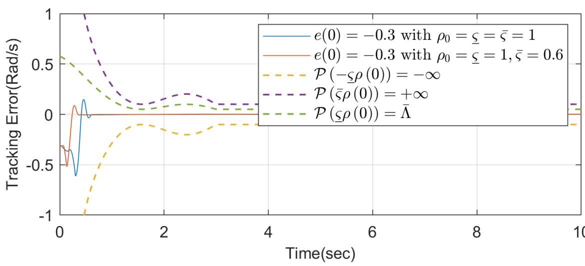

Fig. 6. Tracking error with Case 3.

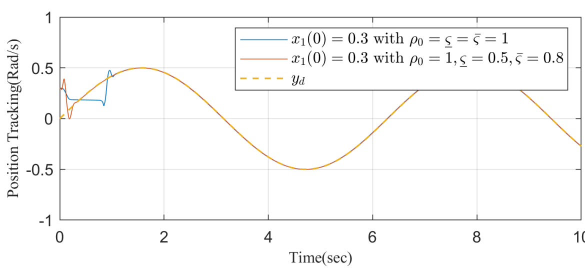

Fig. 7. Tracking trajectory with Case 4.

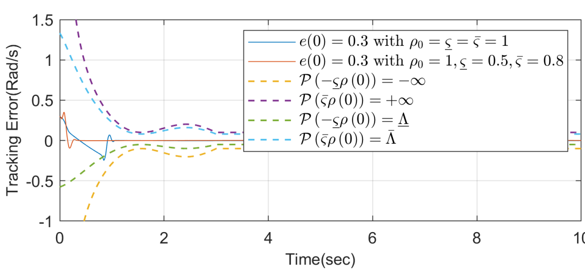

Fig. 8. Tracking error with Case 4.

Figs. 3 and 4 show the effect of adjusting the lower boundary constraint ($\underline{\varsigma}$) on transient behavior (output overshoot) when $e(0)$ is positive (Case 2). Conversely, Figs. 5 and 6 demonstrate the impact of adjusting the upper boundary constraint ($\bar{\varsigma}$) on transient behavior (output overshoot) when $e(0)$ is negative (Case 3). Additionally, Figs. 7 and 8 present the performance behavior when simultaneously adjusting asymmetric lower ($\underline{\varsigma}$) and upper ($\bar{\varsigma}$) boundary constraints (Case 4), further revealing enhanced controllability.

From these six figures, it is evident that the proposed method enables the adjustment of transient performance (output overshoot) by autonomously setting asymmetric constraints. This sets it apart from existing literature [43] and [44] where asymmetric boundaries cannot be configured.

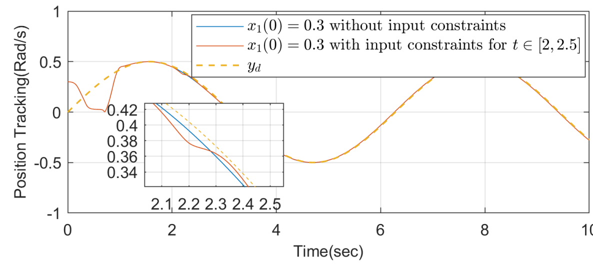

Fig. 9. Tracking trajectory with Case 5.

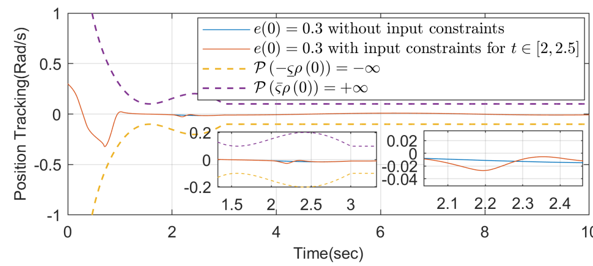

Fig. 10. Tracking error with Case 5.

Figs. 9 and 10 depict the performance behavior of control inputs under short-lived constrained and unconstrained conditions (Case 5). From these two figures, it can be observed that relaxing the boundary constraints during periods $t \in [2, 2.5]$ of constrained control inputs (partial failure) is beneficial, as it ensures the stability of the control system during this interval. Therefore, considering the non-monotonic prescribed performance function is meaningful in practical situations, such as controllers with input saturation [45] and actuator faults [42].

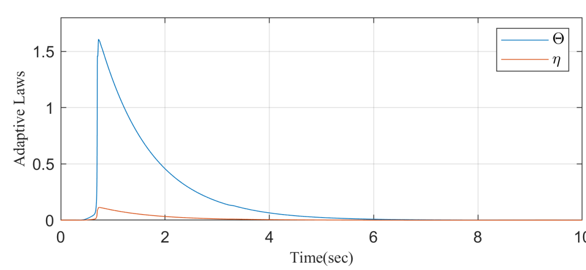

Fig. 11. Adaptive parameter estimation curves.

Fig. 11 illustrates the variation of adaptive laws under Case 1 ($x_1(0) = 0.3$). It can be observed from this figure that both Θ and η are bounded, with η capable of compensating for a part of the fuzzy approximation error, thereby enhancing the overall control performance.

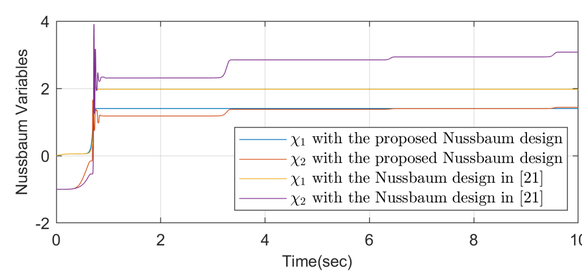

Fig. 12. Nussbaum variable curves.

Fig. 12 shows the variation of the Nussbaum variables in Case 1 ($x_1(0) = 0.3$). It can be noted from this figure that the introduced multiple Nussbaum functions are effective. Compared to the findings in reference [21] ($N(\chi) = \chi^2 \cos(\chi)$), these multiple Nussbaum functions avoid the cancellation of unknown control signs in Lyapunov boundedness analysis. Furthermore, they are applicable to stochastic nonlinear systems with multiple unknown time-varying control coefficients, such as those described in references [30] and [46], unlike reference [21].

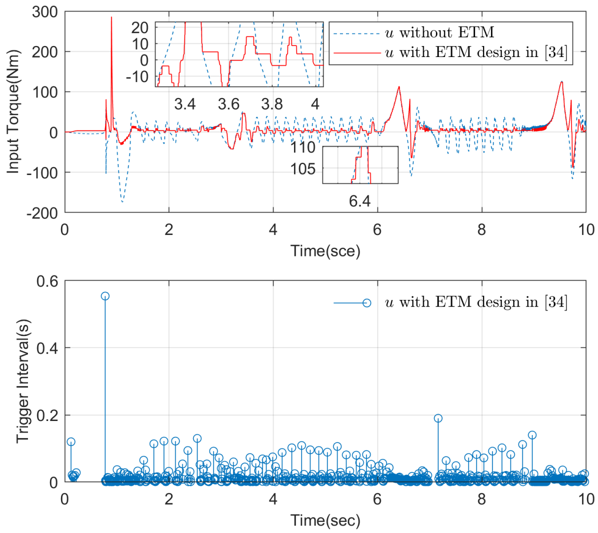

Fig. 13. Control inputs with ETM design in [34]

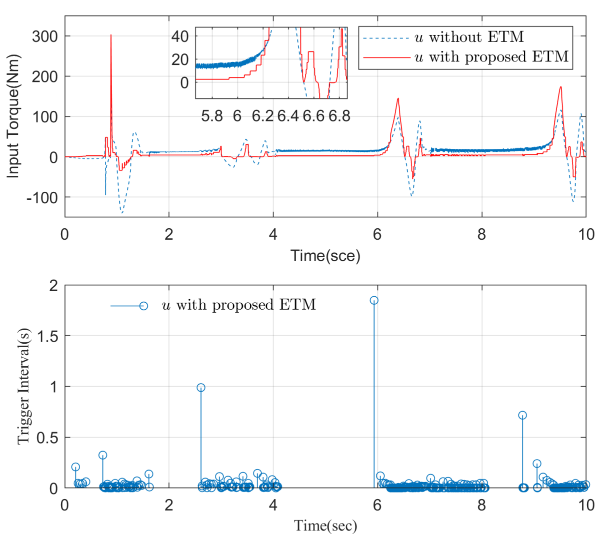

Fig. 14. Control inputs with proposed ETM.

Figs. 13 and 14 present a comparison between the switching thresholds ETM designed in this paper and the classical method [34]. From these figures, it is evident that the proposed ETM is effective and offers more convenient design and adjustment, as it eliminates the robust constraint $\bar{m}_1 > m_1/(1-\delta)$ and $\bar{m}_1 > m_1$.

V. Conclusions

This paper proposes an adaptive fuzzy control for stochastic nonlinear systems with unknown control directions. The proposed scheme provides a versatile design for the prescribed performance function, allowing for convenient switching of prescribed behaviors based on actual applications: (1) Initial errors without any initial condition constraints; (2) Initial errors with lower constraints but no upper constraints; (3) Initial errors with upper constraints but no lower constraints; and (4) Initial errors with simultaneous upper and lower symmetric or asymmetric constraints. The proposed prescribed performance function also exhibit non-monotonicity, which can have a positive impact on controllers with input constraints. Moreover, we introduce a novel class of switching threshold ETM. This ETM eliminates the inequality constraints on design parameters present in existing ETMs while also possessing the capability to balance triggering frequency and control accuracy. Furthermore, we introduce a class of multiple Nussbaum functions to handle unknown control directions, thus avoiding the issue of multiple variables cancelling each other out, while also broadening their application in stochastic nonlinear systems. Simultaneously, the integration of the single-parameter estimation method helps to reduce the computational burden of adaptive parameters. The simulation results confirm the effectiveness and superiority of the control scheme.

The research in this paper has the following limitation: although the non-monotonic prescribed performance function can achieve non-monotonic changes in local regions, it heavily relies on the monotonicity of the rate function $r(t)$. Therefore, accurately designing and adjusting non-monotonic intervals is very challenging.

A future research direction involves integrating the rate function $r(t)$ and piece-wise continuous stretching functions similar to [47], enabling custom adjustment of non-monotonic intervals.

Appendix

Proof of Theorem 1: Define $P(t) = V(t)e^{\sigma t}$, one has $\mathrm{E}[P(t)]|_0^t = \mathrm{E}\left[\int_0^t \mathcal{L}P(\tau)\,d\tau\right]$ and $\mathrm{E}[V(t)] = \mathrm{E}\left[\int_0^t \mathcal{L}V(\tau)\,d\tau\right]$. Note that $\mathcal{L}P(t) = \sigma V(t)e^{\sigma t} + \mathcal{L}V(t)e^{\sigma t}$, then we can obtain

$$\begin{aligned}&\mathrm{E}[P(t)]|_0^t = \int_0^t \left[\sigma V(\tau)e^{\sigma\tau} + \mathcal{L}V(\tau)e^{\sigma\tau}\right]d\tau\\&\leq \int_0^t \left\{\sum_{i=1}^n \left[b_i(\tau)N_i(\chi_i(\tau)) + 1\right]\dot{\chi}_i(\tau) + \beta\right\}e^{\sigma\tau}d\tau.\end{aligned} \tag{48}$$

From the right hand side of (48), one has

$$\begin{aligned}&\int_0^t \left\{\sum_{i=1}^n \left[b_i(\tau)N_i(\chi_i(\tau)) + 1\right]\dot{\chi}_i(\tau) + \beta\right\}e^{\sigma\tau}d\tau\\&\leq \int_0^t \sum_{i=1}^n \left[b_i(\tau)N_i(\chi_i(\tau)) + 1\right]\dot{\chi}_i(\tau)e^{\sigma\tau}d\tau + \frac{\beta}{\sigma}\left(e^{\sigma t} - 1\right).\end{aligned} \tag{49}$$

Substituting (49) into (48) yields

$$\begin{aligned}&\mathrm{E}[P(t)] - \mathrm{E}[P(0)]\\&\leq \int_0^t \sum_{i=1}^n \left[b_i(\tau)N_i(\chi_i(\tau)) + 1\right]\dot{\chi}_i(\tau)e^{\sigma\tau}d\tau + \frac{\beta}{\sigma}\left(e^{\sigma t} - 1\right),\end{aligned} \tag{50}$$

which implies that

$$\begin{aligned}&\mathrm{E}\left[V\left(t\right)\right]\le\int\limits_0^t\sum_{i=1}^n\dot{\chi}_i\left(\tau\right)e^{-\sigma(t-\tau)}d\tau+\mathrm{E}\left[V\left(0\right)\right]e^{-\sigma t}\\&+\int\limits_0^t\sum_{i=1}^n b_i\left(\tau\right)N_i\left(\chi_i\left(\tau\right)\right)\dot{\chi}_i\left(\tau\right)e^{-\sigma(t-\tau)}d\tau+\tfrac{\beta}{\sigma}\left(1-e^{-\sigma t}\right).\end{aligned}\tag{51}$$

Next, we prove $\chi_i\left(t\right), i=1,\ldots,j,\ldots,n$ are bounded in probability by contradiction. We assume that $\chi_1\left(t\right),\ldots,\chi_j\left(t\right)$ are unbounded in probability and $\chi_{j+1}\left(t\right),\ldots,\chi_n\left(t\right)$ are bounded in probability, then, from (51), we can obtain

$$\mathrm{E}\left[V\left(t\right)\right]\le\mathrm{E}\left[V\left(0\right)\right]e^{-\sigma t}+\frac{\beta}{\sigma}\left(1-e^{-\sigma t}\right)+Q\left(t\right)+C_1,\tag{52}$$

where

$$\begin{aligned}&C_1=\sum_{i=j+1}^n\int\limits_0^t\dot{\chi}_i\left(\tau\right)e^{-\sigma(t-\tau)}d\tau\\&+\sum_{i=j+1}^n\int\limits_0^t b_i\left(\tau\right)N_i\left(\chi_i\left(\tau\right)\right)\dot{\chi}_i\left(\tau\right)e^{-\sigma(t-\tau)}d\tau,\\&Q\left(t\right)=\int\limits_0^t\sum_{i=1}^j\dot{\chi}_i\left(\tau\right)e^{-\sigma(t-\tau)}d\tau\\&+\int\limits_0^t\sum_{i=1}^j\left|b_i\left(\tau\right)\right|\mathrm{sign}\left[b_i\left(\tau\right)\right]N_i\left[\chi_i\left(\tau\right)\right]\dot{\chi}_i\left(\tau\right)e^{-\sigma(t-\tau)}d\tau.\end{aligned}\tag{53}$$

From (53), we know that the unboundedness or boundedness of $\chi_i\left(t\right)$ implies the unboundedness or boundedness of $Q\left(t\right)$. Therefore, we discuss the following two cases:

Case 1. $\chi_i\left(t\right), i=1,\ldots,j$ have no upper bound.

First, define three monotonically increasing sequences $\left\{\Gamma_{1,i,p}\right\}_{p=1}^{\infty}$, $\left\{\Gamma_{2,i,p}\right\}_{p=1}^{\infty}$, and $\left\{\Gamma_{3,i,p}\right\}_{p=1}^{\infty}$ as $\Gamma_{1,i,p}=(4p-1)\,\pi/2^i+\nu_i\pi$, $\Gamma_{2,i,p}=(4p-1)\,\pi/2^i+\nu_i\pi+\theta_i/2^{i-1}$, and $\Gamma_{3,i,p}=(4p+1)\,\pi/2^i+\nu_i\pi-\theta_i/2^{i-1}$, where $0\le\theta_i\le\pi/2$, and $\nu_i=\sum_{m=1}^i\left[2^{-m}+2^{-m}\mathrm{sign}\left(b_m\right)\right]\ge0$. Then, we can obtain

$$\begin{aligned}&2^{i-1}\nu_i=2^{i-1}\sum_{m=1}^i\left[2^{-m}+2^{-m}\mathrm{sign}\left(b_m\right)\right]\\&=2^{i-1}\sum_{m=1}^{i-1}\left[2^{-m}+2^{-m}\mathrm{sign}\left(b_m\right)\right]+\tfrac{1}{2}\left[1+\mathrm{sign}\left(b_i\right)\right].\end{aligned}\tag{54}$$

From (54), when $\mathrm{sign}\left(b_i\right)=-1$, $2^{i-1}\nu_i$ are positive even integers, when $\mathrm{sign}\left(b_i\right)=1$, $2^{i-1}\nu_i$ are positive odd integers. Define three increasing time sequences $\left\{t_{1,i,p}\right\}_{p=1}^{\infty}$, $\left\{t_{2,i,p}\right\}_{p=1}^{\infty}$, and $\left\{t_{3,i,p}\right\}_{p=1}^{\infty}$ as $\chi_i\left(t_{1,i,p}\right)=\Gamma_{1,i,p}$, $\chi_i\left(t_{2,i,p}\right)=\Gamma_{2,i,p}$, and $\chi_i\left(t_{3,i,p}\right)=\Gamma_{3,i,p}$. From the above discussion, it is easy to know that $\lim_{p\to\infty}t_{1,i,p}=\lim_{p\to\infty}t_{2,i,p}=\lim_{p\to\infty}t_{3,i,p}=T_f$, and $\lim_{p\to\infty}\Gamma_{1,i,p}=\lim_{p\to\infty}\Gamma_{2,i,p}=\lim_{p\to\infty}\Gamma_{3,i,p}=\infty$. Then, we can obtain

$$\begin{aligned}&Q\left(t\right)\le\bar{Q}\left(t\right)\\&=\sum_{i=1}^j\int\limits_{t_{2,i,p}}^{t_{3,i,p}}\left|b_i\right|\mathrm{sign}\left(b_i\right)N_i\left(\chi_i\right)\dot{\chi}_ie^{-\sigma(t_{3,i,p}-\tau)}d\tau\\&+\sum_{i=1}^j\int\limits_{t_{1,i,p}}^{t_{2,i,p}}\left|b_i\right|\mathrm{sign}\left(b_i\right)N_i\left(\chi_i\right)\dot{\chi}_ie^{-\sigma(t_{3,i,p}-\tau)}d\tau\\&+\sum_{i=1}^j\int\limits_0^{t_{1,i,p}}\left|b_i\right|\mathrm{sign}\left(b_i\right)N_i\left(\chi_i\right)\dot{\chi}_ie^{-\sigma(t_{3,i,p}-\tau)}d\tau\\&+\sum_{i=1}^j\int\limits_0^{t_{3,i,p}}\dot{\chi}_ie^{-\sigma(t_{3,i,p}-\tau)}d\tau+C_1.\end{aligned}\tag{55}$$

Taking integration over the interval $[0,\Gamma_{1,i,p}]$, one has

$$\begin{aligned}&\int\limits_0^{\Gamma_1}\mathrm{sign}\left(b_i\right)N_i\left(\chi_i\right)d\chi_i\\&=\mathrm{sign}\left(b_i\right)\left[\cos\left(\Gamma_{1,i,p}\right)-1\right]\cos\left(2p\pi-\tfrac{1}{2}\pi+2^{i-1}\nu_i\pi\right),\end{aligned}\tag{56}$$

where $2^{i-1}\nu_i$ are positive integers in (54). Then, we have $\int_0^{\Gamma_1}\mathrm{sign}\left(b_i\right)N_i\left(\chi_i\right)d\chi_i=0$. Similar to (56), we can know that $\int_0^{(4p+1)\pi/2^i+\nu_i\pi}\mathrm{sign}\left(b_i\right)N_i\left(\chi_i\right)d\chi_i=0$, and

$$\begin{aligned}&\int\limits_0^{\frac{p\pi}{2^{i-2}}+\nu_i\pi}\mathrm{sign}\left(b_i\right)N_i\left(\chi_i\right)d\chi_i\\&=\mathrm{sign}\left(b_i\right)\cos\left(2^{i-1}\nu_i\pi\right)\left\{\cosh\left[\left(\tfrac{p\pi}{2^{i-2}}+\nu_i\pi\right)^2\right]-1\right\}<0.\end{aligned}\tag{57}$$

Define intervals $I_{i,0}$, $I_{i,1}$, $I_{i,2}$, …, $I_{i,2p}$ as $I_{i,0}=\left[\nu_i\pi,\pi/2^i+\nu_i\pi\right]$, $I_{i,1}=\left[\pi/2^i+\nu_i\pi,3\pi/2^i+\nu_i\pi\right]$, $I_{i,2}=\left[3\pi/2^i+\nu_i\pi,5\pi/2^i+\nu_i\pi\right]$, …, $I_{i,2p}=\left[(4p-1)\,\pi/2^i+\nu_i\pi,(4p+1)\,\pi/2^i+\nu_i\pi\right]$. Define instants $\bar{\eth}_0$, $\underline{\eth}$, $\eth_{i,0}$, $\eth_{i,1}$, $\eth_{i,2}$, …, $\eth_{i,2p}$ as $\chi_i\left(\bar{\eth}_0\right)=\pi/2$, $\chi_i\left(\underline{\eth}\right)=\nu_i\pi$, $\chi_i\left(\eth_{i,0}\right)=\pi/2^i+\nu_i\pi$, $\chi_i\left(\eth_{i,1}\right)=3\pi/2^i+\nu_i\pi$, $\chi_i\left(\eth_{i,2}\right)=5\pi/2^i+\nu_i\pi$, …, $\chi_i\left(\eth_{i,2p}\right)=(4p+1)\,\pi/2^i+\nu_i\pi$. According to the properties of cos-functions, we can know that $\int_0^{\chi_i}\mathrm{sign}\left(b_i\right)N_i\left(\tau\right)d\tau$ should be non-positive within the interval $I_{i,2p}$. Then, we can derive the first term of $\bar{Q}\left(t\right)$ as

$$\begin{aligned}&\sum_{i=1}^j\int\limits_{t_{2,i,p}}^{t_{3,i,p}}b_iN_i\left(\chi_i\right)\dot{\chi}_ie^{-\sigma(t_{3,i,p}-\tau)}d\tau\\&\le\sum_{i=1}^j e^{-\sigma(t_{3,i,p}-t_{2,i,p})}\int\limits_{\Gamma_{2,i,p}}^{\Gamma_{3,i,p}}\left|b_i\right|\mathrm{sign}\left(b_i\right)N_i\left(\chi_i\right)d\chi_i\\&\le-\sum_{i=1}^j B_{\min}e^{-\sigma(t_{3,i,p}-t_{2,i,p})}\sin\left(\theta_i\right)\diamondsuit,\end{aligned}\tag{58}$$

where $B_{\min}=\min\limits_i\underline{b}_i$, and $\diamondsuit=\cosh\left(\Gamma_{3,i,p}^2\right)+\cosh\left(\Gamma_{2,i,p}^2\right)$.

Then, the second part of $\bar{Q}\left(t\right)$ can be derived as

$$\begin{aligned}&\sum_{i=1}^j\int\limits_{t_{1,i,p}}^{t_{2,i,p}}\left|b_i\right|\mathrm{sign}\left(b_i\right)N_i\left(\chi_i\right)\dot{\chi}_ie^{-\sigma(t_{3,i,p}-\tau)}d\tau\\&\le B_{\min}\sum_{i=1}^j e^{-\sigma(t_{2,i,p}-t_{1,i,p})}\int\limits_{\Gamma_{1,i,p}}^{\Gamma_{2,i,p}}\mathrm{sign}\left(b_i\right)N_i\left(\chi_i\right)d\chi_i\le0.\end{aligned}\tag{59}$$

As for the the third part of $\bar{Q}\left(t\right)$, we obtain that $\int_{\eth_{i,q-1}}^{\eth_{i,q}}\mathrm{sign}\left(b_i\right)N_i\left(\chi_i\right)\dot{\chi}_ie^{-\sigma(\eth_{i,q}-\tau)}d\tau\le0$, $q=1,2,\ldots,2p-1$, within the interval $[\eth_{i,q-1},\eth_{i,q}]$. Moreover, we can obtain that $\int_0^{\pi/2}\mathrm{sign}\left(b_i\right)N_i\left(\chi_i\right)d\chi_i=0$, which implies that

if $b_i>0$, then one has

$$\begin{aligned}&\int\limits_0^{\bar{\eth}_0}\mathrm{sign}\left(b_i\right)N_i\left(\chi_i\right)\dot{\chi}_ie^{-\sigma(\underline{\eth}-\tau)}d\tau\\&\le\int\limits_0^{\bar{\eth}_0}\mathrm{sign}\left(b_i\right)N_i\left(\chi_i\right)\dot{\chi}_id\tau=0,\end{aligned}\tag{60}$$

if $b_i<0$, then one has

$$\begin{aligned}&\int\limits_0^{\bar{\eth}_0}\mathrm{sign}\left(b_i\right)N_i\left(\chi_i\right)\dot{\chi}_ie^{-\sigma(\underline{\eth}-\tau)}d\tau\\&\le e^{-\sigma\left(\underline{\eth}-\bar{\eth}_0\right)}\int\limits_0^{\bar{\eth}_0}\mathrm{sign}\left(b_i\right)N_i\left(\chi_i\right)\dot{\chi}_id\tau=0.\end{aligned}\tag{61}$$

From (60) and (61), we know that $\int_0^{\underline{\eth}} \operatorname{sign}(b_i) N_i(\chi_i) \dot{\chi}_i e^{-\sigma(\underline{\eth}-\tau)} d\tau \leq 0$. Then, the third part of $\bar{Q}(t)$ can be derived as

$$\begin{aligned} &\sum_{i=1}^{j} \int_{0}^{t_{1,i,p}} b_i N_i(\chi_i) \dot{\chi}_i e^{-\sigma(t_{3,i,p}-\tau)} d\tau \\ &\leq \sum_{q=1}^{2p-1} \sum_{i=1}^{j} \underline{b}_i \int_{\eth_{i,q-1}}^{\eth_{i,q}} \operatorname{sign}(b_i) N_i(\chi_i) \dot{\chi}_i e^{-\sigma(\eth_{i,q}-\tau)} d\tau \\ &+ \sum_{i=1}^{j} \underline{b}_i \int_{0}^{\underline{\eth}} \operatorname{sign}(b_i) N_i(\chi_i) e^{-\sigma(\nu_i \pi-\tau)} d\tau \leq 0. \end{aligned} \tag{62}$$

Then, the fourth part of $\bar{Q}(t)$ satisfies

$$\sum_{i=1}^{j} \int_{0}^{t_{3,i,p}} e^{-\sigma(t_{3,i,p}-\tau)} \dot{\chi}_i d\tau \leq \sum_{i=1}^{j} \Gamma_{3,i,p} - \sum_{i=1}^{j} \chi_i(0). \tag{63}$$

From (60)–(63), (55) can be rewritten as

$$\begin{aligned} Q(t) \leq &-B_{\min} \sum_{i=1}^{j} \sin(\theta_i) \left[\cosh\left(\Gamma_{3,i,p}^2\right) + \cosh\left(\Gamma_{2,i,p}^2\right)\right] \\ &+ \sum_{i=1}^{j} \Gamma_{3,i,p} - \sum_{i=1}^{j} \chi_i(0) + C_1, \end{aligned} \tag{64}$$

which is equivalent to

$$Q(t) \leq -\sum_{i=1}^{j} C_3 \cosh\left(\Gamma_{3,i,p}^2\right) C_4 + C_2, \tag{65}$$

where $C_2 = -\sum_{i=1}^{j} \chi_i(0) + C_1$, $C_3 = B_{\min} \sin(\theta_i)$, and $C_4 = 1 + \cosh\left(\Gamma_{2,i,p}^2\right) / \cosh\left(\Gamma_{3,i,p}^2\right) + \Gamma_{3,i,p} / \left[C_3 \cosh\left(\Gamma_{3,i,p}^2\right)\right]$. From (65), we have $\lim_{t \to T_f} Q(t) = -\infty$, which contradicts $Q(t) \geq 0$. Hence, $\chi_i(t), i = 1, \ldots, j$ have upper bound on $[0, T_f)$.

Case 2. $\chi_i(t), i = 1, \ldots, j$ have no lower bound.

Consider that $\chi_i(t), i = 1, \ldots, j$ have no lower bound on $[0, T_f)$, which means that $-\chi_i$ have no upper bound on $[0, T_f)$. Due to the fact that $\int_0^{\chi_i} \operatorname{sign}(b_i) N_i(\tau) d\tau$ is an even function, $Q(t)$ should satisfy

$$Q(t) \leq -\sum_{i=1}^{j} D_3 \cosh\left(\Gamma_{3,i,p}^2\right) D_4 + D_2, \tag{66}$$

where $D_1 = \sum_{i=j+1}^{k} \int_0^t b_i(\tau) N_i[\chi_i(\tau)] \dot{\chi}_i(\tau) e^{-\sigma(t-\tau)} d\tau - \sum_{i=j+1}^{k} \int_0^t e^{-\sigma(t-\tau)} \dot{\chi}_i(\tau) d\tau$, $D_2 = \sum_{i=1}^{j} \chi_i(0) + D_1$, $D_3 = B_{\min} e^{-\sigma(t_{3,i,p}-t_{2,i,p})} \sin(\theta_i)$, and $D_4 = 1 + \cosh\left(\Gamma_{2,i,p}^2\right) / \cosh\left(\Gamma_{3,i,p}^2\right) + \Gamma_{3,i,p} / \left[D_3 \cosh\left(\Gamma_{3,i,p}^2\right)\right]$. From (66), we have $\lim_{t \to T_f} Q(t) = -\infty$, which contradicts $Q(t) \geq 0$. Hence, $\chi_i(t), i = 1, \ldots, j$ have lower bound on $[0, T_f)$.

According to the above discussion, we can conclude that $\chi_i(t), i = 1, \ldots, j$ are bounded in probability on $[0, T_f)$. Therefore, $V(t)$ is also bounded in probability on $[0, T_f)$. Then, due to the fact that $\sum_{i=1}^{n} [b_i(t) N_i(\chi_i) + 1] \dot{\chi}_i$ is integrable, we obtain that $|\sum_{i=1}^{n} [b_i(t) N_i(\chi_i) + 1] \dot{\chi}_i| \leq \bar{N}$ on $[0, T_f)$ with $\bar{N}$ being a constant. At this stage, we have presented the complete proof of Theorem 1.

References

[1] J. Zhang, W. Jiang and S. S. Ge, "Adaptive Fuzzy Control for Uncertain Strict-Feedback Nonlinear Systems With Full-State Constraints Using Disturbance Observer," *IEEE Transactions on Systems, Man, and Cybernetics: Systems*, vol. 53, no. 10, pp. 6145-6156, Oct. 2023.

[2] P. Wan and Z. Zeng, "Adaptive Tracking Control of State-Constrained Strict-Feedback Nonlinear Systems Using Direct Method," *IEEE Transactions on Systems, Man, and Cybernetics: Systems*, vol. 53, no. 8, pp. 5116-5126, Aug. 2023.

[3] H. Wang, K. Xu and H. Zhang, "Adaptive Finite-Time Tracking Control of Nonlinear Systems With Dynamics Uncertainties," *IEEE Transactions on Automatic Control*, vol. 68, no. 9, pp. 5737-5744, Sep. 2023.

[4] J. Zhang, Y. Fu and J. Fu, "Adaptive Finite-Time Optimal Formation Control for Second-Order Nonlinear Multiagent Systems," *IEEE Transactions on Systems, Man, and Cybernetics: Systems*, vol. 53, no. 10, pp. 6132-6144, Oct. 2023.

[5] H. Wang, M. Chen, and X. Liu. "Fuzzy Adaptive Fixed-time Quantized Feedback Control for a Class of Nonlinear Systems," *ACTA Automatica Sinica*, vol. 47, no. 12, pp. 2823-2830, Dec. 2021.

[6] H. Ren, H. Ma, H. Li and Z. Wang, "Adaptive Fixed-Time Control of Nonlinear MASs With Actuator Faults," *IEEE/CAA Journal of Automatica Sinica*, vol. 10, no. 5, pp. 1252-1262, May 2023.

[7] L. Liu and M. Kong, "A New Design Method to Global Asymptotic Stabilization of Strict-Feedforward Stochastic Nonlinear Time Delay Systems," *Automatica*, vol. 151, no. 110932, May 2023.

[8] Y. Zhao and Q. Zhu, "Stabilization of Stochastic Highly Nonlinear Delay Systems With Neutral Term," *IEEE Transactions on Automatic Control*, vol. 68, no. 4, pp. 2544-2551, Apr. 2023.

[9] C. Zhao and Y. Zhang, "Understanding the Capability of PD Control for Uncertain Stochastic Systems," *IEEE Transactions on Automatic Control*, vol. 69, no. 1, pp. 495-502, Jan. 2024.

[10] Y. Sun, C. Liu, H. Wang, C. Li and Y. Zhou, "A Novel Adaptive Controller for Nonlinear Stochastic Systems With Uncertain Virtual Control Gains and Input Nonlinearities," *IEEE Transactions on Systems, Man, and Cybernetics: Systems*, vol. 53, no. 12, pp. 7595-7607, Dec. 2023.

[11] Y. Yuan, J. Zhao, Z. Y. Sun and X. Xie, "Practically Fast Finite-Time Stability in the Mean Square of Stochastic Nonlinear Systems: Application to One-Link Manipulator," *IEEE Transactions on Systems, Man, and Cybernetics: Systems*, vol. 54, no. 1, pp. 312-323, Jan. 2024.

[12] J. Lee, W. M. Haddad and M. Lanchares, "Finite Time Stability and Optimal Finite Time Stabilization for Discrete-Time Stochastic Dynamical Systems," *IEEE Transactions on Automatic Control*, vol. 68, no. 7, pp. 3978-3991, Jul. 2023.

[13] Y. Xia, K. Xiao, Y. Yao, Z. Geng and Z. Lendek, "Fixed-Time Fuzzy Vibration Reduction for Stochastic MEMS Gyroscopes With Low Communication Resources," *IEEE Transactions on Fuzzy Systems*, vol. 32, no. 8, pp. 4220-4233, Aug. 2024.

[14] K. Xu, H. Wang and P. X. Liu, "Adaptive Fixed-Time Control for High-Order Stochastic Nonlinear Time-Delay Systems: An Improved Lyapunov–Krasovskii Function," *IEEE Transactions on Cybernetics*, vol. 54, no. 2, pp. 776-786, Feb. 2024.

[15] S. P. Bhat and D. S. Bernstein, "Continuous finite-time stabilization of the translational and rotational double integrators," *IEEE Transactions on Automatic Control*, vol. 43, no. 5, pp. 678-682, May. 1998.

[16] A. Polyakov, D. Efimov, and W. Perruquetti, "Finite-time and fixed-time stabilization: Implicit Lyapunov function approach," *Automatica*, vol. 51, pp. 332-340, Jan. 2015.

[17] T. Zhang, S. F. Su, W. Wei and R. H. Yeh, "Practically Predefined-Time Adaptive Fuzzy Tracking Control for Nonlinear Stochastic Systems," *IEEE Transactions on Cybernetics*, vol. 53, no. 12, pp. 8000-8012, Dec. 2023.

[18] P. Zarchan, Tactical and Strategic Missile Guidance, 6th ed. Reston, VA, USA: AIAA, 2012.

[19] Y. Xia, Z. Geng, and K. Xiao, "Event-Based Adaptive Fuzzy Control for Stochastic Nonlinear Systems with Prescribed Performance," *Chaos Solitons & Fractals*, vol. 180, no. 114501, Mar. 2024.

[20] Y. Song, H. Ye and F. L. Lewis, "Prescribed-Time Control and Its Latest Developments," *IEEE Transactions on Systems, Man, and Cybernetics: Systems*, vol. 53, no. 7, pp. 4102-4116, Jul. 2023.

[21] K. Zhao, Y. Song, C. L. P. Chen and L. Chen, "Adaptive Asymptotic Tracking With Global Performance for Nonlinear Systems With Unknown Control Directions," *IEEE Transactions on Automatic Control*, vol. 67, no. 3, pp. 1566-1573, Mar. 2022.

[22] D. Zeng, Z. Liu, C. L. P. Chen, Y. Wang, Y. Zhang and Z. Wu, "Adaptive Neural Prescribed-Time Control of Switched Nonlinear Systems With Mode-Dependent Average Dwell Time," *IEEE Transactions on Systems, Man, and Cybernetics: Systems*, vol. 53, no. 12, pp. 7427-7440, Dec. 2023.

[23] C. P. Bechlioulis and G. A. Rovithakis, "Robust Adaptive Control of Feedback Linearizable MIMO Nonlinear Systems With Prescribed Performance," *IEEE Transactions on Automatic Control*, vol. 53, no. 9, pp. 2090-2099, Oct. 2008.

[24] H. Huang, W. He, J. Li, B. Xu, C. Yang and W. Zhang, "Disturbance Observer-Based Fault-Tolerant Control for Robotic Systems With Guaranteed Prescribed Performance," *IEEE Transactions on Cybernetics*, vol. 52, no. 2, pp. 772-783, Feb. 2022.

[25] H. Ma, Q. Zhou, H. Li and R. Lu, "Adaptive Prescribed Performance Control of A Flexible-Joint Robotic Manipulator With Dynamic Uncertainties," *IEEE Transactions on Cybernetics*, vol. 52, no. 12, pp. 12905-12915, Dec. 2022.

[26] T. Berger, "Fault-Tolerant Funnel Control for Uncertain Linear Systems," *IEEE Transactions on Automatic Control*, vol. 66, no. 9, pp. 4349-4356, Sep. 2021.

[27] R. Nussbaum, "Some Remarks on a Conjecture in Parameter Adaptive Control," *Systems & Control Letters*, vol. 3, no. 5, pp. 243-246, 1983.

[28] J. Zhang, Q. Wang and W. Ding, "Global Output-Feedback Prescribed Performance Control of Nonlinear Systems With Unknown Virtual Control Coefficients," *IEEE Transactions on Automatic Control*, vol. 67, no. 12, pp. 6904-6911, Dec. 2022.

[29] C. Hua, Z. Sun and Z. Chen, "Exponential Stabilization for Time-Delay Nonlinear Interconnected Systems With Unknown Control Directions and Unmodeled Dynamics," *IEEE Transactions on Systems, Man, and Cybernetics: Systems*, vol. 53, no. 7, pp. 3979-3989, Jul. 2023.

[30] J. Xia, Y. Lian, S. F. Su, H. Shen and G. Chen, "Observer-Based Event-Triggered Adaptive Fuzzy Control for Unmeasured Stochastic Nonlinear Systems With Unknown Control Directions," *IEEE Transactions on Cybernetics*, vol. 52, no. 10, pp. 10655-10666, Oct. 2022.

[31] J. Huang, W. Wang, C. Wen, and J. Zhou, "Adaptive Control of A Class of Strict-Feedback Time-Varying Nonlinear Systems with Unknown Control Coefficients," *Automatica*, vol. 93, pp. 98–105, Jul. 2018.

[32] Z. Liu, J. Huang, C. Wen and X. Su, "Distributed Control of Nonlinear Systems With Unknown Time-Varying Control Coefficients: A Novel Nussbaum Function Approach," *IEEE Transactions on Automatic Control*, vol. 68, no. 7, pp. 4191-4203, Jul. 2023.

[33] Y. Liu, H. Zhang, Y. Wang, H. Ren and Q. Li, "Adaptive Fuzzy Prescribed Finite-Time Tracking Control for Nonlinear System With Unknown Control Directions," *IEEE Transactions on Fuzzy Systems*, vol. 30, no. 6, pp. 1993-2003, Jun. 2022.

[34] L. Xing, C. Wen, Z. Liu, H. Su and J. Cai, "Event-Triggered Adaptive Control for a Class of Uncertain Nonlinear Systems," *IEEE Transactions on Automatic Control*, vol. 62, no. 4, pp. 2071-2076, Apr. 2017.

[35] H. Ma, H. Ren, Q. Zhou, H. Li and Z. Wang, "Observer-Based Neural Control of N -Link Flexible-Joint Robots," *IEEE Transactions on Neural Networks and Learning Systems*, doi: 10.1109/TNNLS.2022.3203074.

[36] B. Li, J. Xia, S. F. Su, W. Sun and H. Zhang, "Event-Triggered Adaptive Fuzzy Tracking Control for Nonlinear Systems With Unknown Control Directions," *IEEE Transactions on Systems, Man, and Cybernetics: Systems*, vol. 52, no. 7, pp. 4648-4657, Jul. 2022.

[37] Y. Xia, C. Liu, Y. Tuo, and J. Li, "Command Filter-Based Event-Triggered Control for Stochastic MEMS Gyroscopes with Finite-Time Prescribed Performance," ISA Transactions, vol. 148, pp. 212-223, May 2024.

[38] G. Chen, Q. Zhou, H. Li, D. Yao and C. K. Ahn, "Event-Triggered State Estimation and Control for Networked Nonlinear Systems Under Dynamic Sparse Attacks," *IEEE Transactions on Network Science and Engineering*, vol. 11, no. 2, pp. 1947-1958, Mar-Apr. 2024.

[39] Z. Ma and P. Huang, "Adaptive Neural-Network Controller for an Uncertain Rigid Manipulator With Input Saturation and Full-Order State Constraint," *IEEE Transactions on Cybernetics*, vol. 52, no. 5, pp. 2907-2915, May 2022.

[40] Y. Ren, Z. Zhao, C. K. Ahn and H. Li, "Adaptive Fuzzy Control for an Uncertain Axially Moving Slung-Load Cable System of a Hovering Helicopter With Actuator Fault," *IEEE Transactions on Fuzzy Systems*, vol. 30, no. 11, pp. 4915-4925, Nov. 2022.

[41] X. Bu, M. Lv, H. Lei and J. Cao, "Fuzzy Neural Pseudo Control With Prescribed Performance for Waverider Vehicles: A Fragility-Avoidance Approach," *IEEE Transactions on Cybernetics*, vol. 53, no. 8, pp. 4986-4999, Aug. 2023.

[42] P. Yang, Y. Su, and L. Zhang, "Proximate Fixed-Time Fault-Tolerant Tracking Control for Robot Manipulators with Prescribed Performance," *Automatica*, vol. 157, no. 111262, Nov. 2023.

[43] F. Wu, J. Lian, D. Wang and G. Zhai, "Prescribed Performance Bumpless Transfer Control for Switched Large-Scale Nonlinear Systems," *IEEE Transactions on Systems, Man, and Cybernetics: Systems*, vol. 53, no. 8, pp. 5139-5148, Aug. 2023.

[44] X. Bu, B. Jiang and H. Lei, "Low-Complexity Fuzzy Neural Control of Constrained Waverider Vehicles via Fragility-Free Prescribed Performance Approach," *IEEE Transactions on Fuzzy Systems*, vol. 31, no. 7, pp. 2127-2139, July 2023.

[45] H. Xie, G. Zong, D. Yang, X. Zhao and Y. Yi, "Flexible-Fixed-Time-Performance-Based Adaptive Asymptotic Tracking Control of Switched Nonlinear Systems With Input Saturation," *IEEE Transactions on Automation Science and Engineering*, doi: 10.1109/TASE.2023.3324953.

[46] Y. Liu and H. Ma, "Adaptive Fuzzy Tracking Control of Nonlinear Switched Stochastic Systems With Prescribed Performance and Unknown Control Directions," *IEEE Transactions on Systems, Man, and Cybernetics: Systems*, vol. 50, no. 2, pp. 590-599, Feb. 2020.

[47] Y. Yao, Y. Kang, Y. Zhao, P. Li and J. Tan, "A Novel Prescribed-Time Control Approach of State-Constrained High-Order Nonlinear Systems," *IEEE Transactions on Systems, Man, and Cybernetics: Systems*, doi: 10.1109/TSMC.2024.3352905.

[48] A. Levant, "Higher-Order Sliding Modes, Differentiation and Output-Feedback Control," *International Journal of Control*, Vol. 76, no. 9-10, pp. 924-941, Jun-Jul. 2003.

Yu Xia (Member IEEE) received his Ph.D. degree in mechanical engineering from Chongqing University, Chongqing, China, in 2024. He is currently a Research Fellow in the State Key Laboratory of Mechanical System and Vibration, School of Mechanical Engineering, Shanghai Jiao Tong University, Shang hai, China. His research interests include prescribed performance control, stochastic system control, and electromechanical system control.

Zsófia Lendek (Member IEEE) received the M.Sc. degree degree in control engineering from the Technical University of Cluj-Napoca, Romania, in 2003, the Ph.D. degree from the Delft University of Technology, the Netherlands, in 2009; and her habilitation degree from the Technical University of Cluj-Napoca, Romania, in 2019. She is currently a Full Professor at the Technical University of Cluj-Napoca, Romania. She has previously held research positions in the Netherlands and in France. Her research interests include observer and controller design for nonlinear systems, in particular Takagi-Sugeno fuzzy systems, which adapt the advantages of linear time-invariant system-based design to nonlinear systems, with applications in several fields.

Dr. Lendek is an Associate Editor for IEEE TRANSACTIONS ON FUZZY SYSTEMS and Engineering Applications of Artificial Intelligence and board member of Fuzzy Sets and Systems.

Zhibo Geng received his B.S. and Ph.D. degrees in Mechanical Engineering from Chongqing University, China, in 2015 and 2020, respectively. He is currently a Postdoctoral Researcher at the Department of Aerospace Engineering at the University of Electronic Science and Technology of China in Chengdu, Sichuan Province, China. His research interests are in the areas of mechanical design, gear dynamics, nonlinear dynamics, and control.

Junyang Li received his B.Eng. and Ph.D. degrees in mechanical engineering from Chongqing University, Chongqing, China, in 2006 and 2012, respectively. From 2013 to 2015, he engaged in postdoctoral research at Chongqing University in the field of adaptive control of dynamic systems. He is currently an Associate Professor with the College of Mechanical and Vehicle Engineering at Chongqing University, Chongqing, China. His research interests include precision transmission and intelligent control in aerospace, industrial robotics, and others.

Jiaxu Wang received his B. Eng. degree in mechanical engineering from Chongqing University, Chongqing, China, in 1984. He currently holds the position of Academic Leader at the State Key Laboratory of Mechanical Transmission at Chongqing University. Additionally, he serves as the Academic Dean of the School of Aerospace Science and Engineering at Sichuan University, a Distinguished Professor at the School of Mechanical and Power Engineering at Chongqing University of Science and Technology, and a Part-Time Professor at the School of Mechanical Engineering at Southwest Jiao Tong University. His research interests include high-performance electromechanical drive and control, aerospace equipment design, and manufacturing theory.

Prof. Wang is a valid candidate for the Chinese Academy of Engineering. He is also a member of the discipline evaluation group of the Academic Degrees Committee of the State Council, a member of the expert review group of the National Natural Science Foundation Committee, the chief expert of the national "863 Plan" theme project, and a member of the national space technology expert group. He has won two National Awards for Science and Technology Progress (ranks number one), one National Award for Technological Invention (ranks number one), and the He Liang He Li Science and Technology Innovation Award.